# A MULTI-SCALAR GLOBAL EVALUATION OF THE IMPACT OF ENSO ON DROUGHTS

Sergio M. Vicente-Serrano[1]*, Juan I. López-Moreno[1], Luis Gimeno[2], Raquel Nieto[2], Enrique Morán-Tejeda[1], Jorge Lorenzo-Lacruz[1], Santiago Beguería[3] and Cesar Azorin-Molina[1]

1) Instituto Pirenaico de Ecología, CSIC (Spanish National Research Council), Campus de Aula Dei, P.O. Box 202, Zaragoza 50080, Spain
2) Environmental Physics Laboratory, Universidade de Vigo, Ourense, Spain
3) Estación Experimental de Aula Dei CSIC (Spanish National Research Council), Zaragoza, Spain.

* svicen@ipe.csic.es

## ABSTRACT

In this study we analyzed the influence of the El Niño-Southern Oscillation (ENSO) phenomenon on drought severity at the global scale. A unique aspect of the analysis is that the ENSO influence was quantified using a multi-scalar drought indicator, which allowed assessment of the role of the ENSO phases on drought types affecting various hydrological, agricultural and environmental systems. The study was based on ENSO composites corresponding to El Niño and La Niña phases, which were obtained from the winter El Niño 3.4 index for the period 1901–2006. Drought was identified in a multi-scalar way using the Standardized Precipitation Evapotranspiration Index (SPEI) and the global SPEIbase dataset. The study revealed the differing impacts of the El Niño and La Niña phases on drought severity, the time scales of droughts, and the period of the year when the ENSO phases explained drought variability worldwide. In large areas of America and eastern Europe the role of ENSO events were evident at the shortest time scales (1–3 months) at the beginning of events, but in areas of South Africa, Australia and Southeast Asia the effects were more obvious some months later, and at longer time scales. We also identified areas where severe drought conditions are associated with more than 70% of ENSO events. The propagation of the drought conditions at longer time-scales (e.g., 6- or 12-months) is not directly determined by the atmospheric circulation response to the SST anomalies, since the SPEI anomalies will be caused by the cumulative dry conditions in some specific months. Knowledge of how these effects differ as a function of the El Niño and La Niña phases, and how they propagate throughout the drought time

scales could aid in the prediction of the expected drought severity associated with the ENSO. Lags detected during the study may help forecasting of dry conditions in some regions up to one year before their occurrence.

**KEYWORDS:** Standardized Precipitation Evapotranspiration Index, predictability, climatic change, atmospheric circulation, Southern Oscillation, El Niño, La Niña

## 1. INTRODUCTION

The El Niño-Southern Oscillation (ENSO) phenomenon is one of the main sources of variability in the Earth's climate (Trenberth, 1997; Kiladis and Díaz, 1989; Halpert and Ropelewski, 1992; Philander and Fedorov, 2003); the extremes of this atmosphere–ocean coupled mode are known as the El Niño and La Niña phases. El Niño phases correspond to ENSO events during which pressure differences across the tropical Pacific Ocean are reduced, and sea surface temperature (SST) anomalies are positive in the central and eastern tropical Pacific Ocean (Philander, 1990). La Niña phases correspond to ENSO events characterized by cold SST and an enhanced sea level pressure gradient from west to east across the tropical Pacific Ocean. These anomalous phases affect the temperature of the atmosphere, and the surface and vertical displacement of wind flows and moisture (Rasmusson and Carpenter, 1982).

Many studies have shown a close relationship between ENSO phenomena and climate variability in tropical and subtropical regions (e.g. Ropelewski and Halpert, 1986, 1987; Redmond and Koch, 1991). During El Niño (La Niña) phases there is increased (decreased) precipitation in the south Pacific Ocean, whereas dry (wet) conditions occur in Australia, Southeast Asia, South Africa and northern South America (Smith and Ropelewski, 1997; Cordery and McCall, 2000; Hendon, 2003; Rouault and Richard, 2005; Brown et al., 2009; Nel, 2009; Villar et al., 2009; Kotawhale, 2010).

The ENSO influence on precipitation is not restricted to the Pacific Ocean. Thus, New et al. (2001) estimated that the ENSO phenomenon causes 6.3% of precipitation variance at the global scale, and

also helps explain the climate variability of northern hemisphere regions, mainly in the north Pacific Ocean and North America (Díaz and Kiladis, 1992; Schonher and Nicholson, 1989; Halpert and Ropelewski, 1992; Trenberth and Guillemot, 1996; Mo and Schemm, 2008), on the European continent (Lloyd-Hughes and Saunders, 2002; Bronnimann et al., 2004; Bronnimann, 2007), and in Turkey (Karabörk et al., 2005; Karabörk and Kahya, 2009), the Sahel (Janicot et al., 1996, 2001) and large areas of central Asia (Nazemosadat and Ghasemi, 2004).

The influence of ENSO events on the global variability of precipitation and temperature are well known. Various studies have described the influence of the ENSO on surface climate. Ropelewski and Halpert (1987) provided the first overview of global precipitation patterns associated with El Niño, and identified the months and regions in which wet and dry conditions are related to El Niño events; their following study (Ropelewski and Halpert, 1996) considered La Niña events. Kiladis and Diaz (1989) analyzed the effects of El Niño and La Niña events on global surface temperature.

Current interest in climate responses to variations in atmospheric circulation is mainly focused on the occurrence of extreme events (e.g. floods, droughts, heat waves) that cause major environmental, social and economic damage. Among natural hydroclimatic hazards, drought is the most damaging because it causes major economic losses (Meehl et al., 2000; UN, 2008), famine (Obasi, 1994; Nicholson, 2001) and negative environmental impacts (e.g. Ciais et al., 2005; Breshears et al., 2005).

Droughts are very difficult complex natural hazards to identify, monitor and analyze because of problems associated with objectively quantifying their characteristics in terms of intensity, magnitude, duration and spatial extent. Consequently, determining drought mechanisms is problematic and it is very difficult to establish their onset, extent and cessation. Moreover, drought is a multi-scalar phenomenon, which adds much complexity to any analysis. McKee et al. (1993) clearly illustrated these characteristics of droughts through consideration of usable water resources, including soil moisture, ground water, snowpack, river discharges and reservoir storages. The time period from the arrival of water inputs to the availability of a given usable water resource varies

considerably. Thus, the time scale over which water deficits accumulate becomes extremely important, and functionally separates hydrological, environmental, agricultural and other types of droughts. Thus, the response of crops, natural vegetation and hydrological systems to drought conditions can vary markedly as a function of the time scale (Ji and Peters, 2003; Vicente-Serrano and López-Moreno, 2005; Patel et al., 2007; Vicente-Serrano, 2007; Khan et al., 2008; Lorenzo-Lacruz et al., 2010; Quiring and Ganesh, 2010). This multi-temporal character makes it difficult to identify clear relationships between atmospheric circulation patterns and drought variability. This difficulty is exacerbated by the lags that commonly occur in the response of climatic conditions to atmospheric circulation events, such as El Niño and La Niña.

Few studies have quantified the influence of ENSO phases on droughts using drought indices, and relatively few regions of the world have been studied. These regions are mainly in the USA (Piechota and Dracup, 1996; Rajagopalan et al., 2000; Balling and Goodrich, 2007; Mo and Schemm, 2008; Mo et al., 2009), but also in Indonesia (D'Arrigo and Wilson, 2008), Canada (Shabbar and Skinner, 2004), New Zealand (Fowler and Adams, 2004), South Africa (Rouault and Richard, 2005), Iran (Nazemosadat and Ghasemi, 2004) and the Iberian Peninsula (Vicente-Serrano, 2005).

Some studies have analyzed the impact of ENSO on droughts at the global scale. Dai et al. (2004) developed a global dataset of the Palmer Drought Severity Index (PDSI) and showed that between 1870 and 2002 the pattern of drought variability representing the drought evolution in large regions of North America and central Eurasia was strongly correlated to the ENSO. Appipatanavis et al. (2009) also related the global PDSI with the ENSO, and showed a strong relationship in the southwestern and northwestern United States, South Africa, northeastern Brazil, central Africa, the Indian subcontinent and Australia. Sheffield et al. (2009) recently used an infiltration capacity model to quantify the global occurrence of droughts for the period 1950–2000. They found robust relationships between the surface area of the world affected by drought and the ENSO variability.

While useful and informative, these global studies did not consider the impact of ENSO on drought at different time scales, and thus its impact on various subsystems of the hydrological cycle.

Vicente-Serrano (2005) used a multi-scalar drought index (the Standardized Precipitation Index) to show that the influence of the El Niño and La Niña phases varies widely across time scales in the Iberian Peninsula; this approach is essential in accurately quantifying the wide variety of impacts related to ENSO variability. Thus, when the atmospheric mechanisms of droughts are studied, differing drought time scales must be considered to have a wide perspective of the hazard implications (López-Moreno and Vicente-Serrano, 2008).

This study is the first global multi-scalar analysis of the ENSO impact on droughts. The purpose was to provide a general picture of drought conditions at various time scales associated with warm (El Niño) and cold (La Niña) ENSO events and the associated physical mechanisms. Establishing robust relationships between the ENSO and the evolution of drought is of great relevance because ENSO is the main source of atmospheric circulation variability at a global scale. Such knowledge will enhance internal prediction (Jin et al., 2008) and facilitate improved prediction of droughts (e.g. Stone et al., 1996; Cordery and McCall, 2000), which will enhance the performance of existing drought early warning and monitoring systems (Svoboda et al., 2002, 2004).

## 2. METHODS

### 2.1. Identification of ENSO events

Composites based on ENSO events are commonly used to analyze the nonlinear influence of the ENSO on world climate (Smith and Ropelewski, 1997; Philip and Van Oldenborgh, 2009) because the composite warm event ENSO anomalies are not the exact inverse of their cold event counterparts (Hoerling et al., 1997).

There is general agreement on use of the El Niño 3.4 to monitor ENSO phenomena and to identify its extreme phases. This index was proposed by Trenberth and Hoar (1996), based on the SST in two selected Pacific Ocean areas, which are key regions for ENSO. The index has been widely applied to

137 monitoring of the effect of ENSO on the global climate system, and also used to identify the extreme
138 phases of the ENSO (Trenberth, 1997). In this study the El Niño and La Niña events were identified
139 using the winter (December–February) El Niño 3.4 index between 1901 and 2006, obtained from the
140 Hadley Centre Sea Surface Temperature data set (Rayner et al., 2003). El Niño events were defined
141 by a winter El Niño 3.4 index > 1, and La Niña events were defined by an index < –1. Based on these
142 criteria the winters of 1903, 1906, 1912, 1919, 1926, 1931, 1941, 1958, 1966, 1969, 1973, 1983,
143 1987, 1992, 1995, 1998 and 2003 were classified as El Niño, and the winters of 1910, 1917, 1934,
144 1943, 1950, 1951, 1956, 1971, 1974, 1976, 1985, 1989, 1999 and 2000 were classified as La Niña.
145 By convention the El Niño and La Niña years were defined as those that correspond to the year when
146 records the months of January and February of the event. The month of December therefore
147 corresponded to the year prior to the ENSO event.
148 We plotted the average and standard deviation values of the El Niño 3.4 index for the entire year of
149 El Niño and La Niña events, and also for the previous year (Fig. 1). Trenberth (1997) carried out an
150 extensive analysis of the ENSO extreme phases using the El Niño 3.4 index, and showed that most
151 events began between March and September. Figure shows that the greatest anomalies for both
152 events (El Niño and La Niña) occurred during the winter months (November–January), but the
153 anomalies in SSTs associated with the events commenced in May of the previous year and extended
154 to May–June in the year of the event. Thus, for La Niña and El Niño phases SST anomalies < –0.75
155 and > 0.5, respectively, were recorded from June of the previous year. Therefore, as the ENSO
156 phases were recorded in the winter months and large anomalies in the SST occurred some months
157 prior to and following these phases, it is reasonable to predict the early influence of ENSO events on
158 drought conditions in some regions, with implications at various time scales. For this reason the
159 drought analyses encompassed the year of the event and most of the preceding year.
160
161 **2.2. Drought data set**

To identify drought conditions we used the Standardized Precipitation Evapotranspiration Index (SPEI), which can be calculated at different time scales and considers the combined effects of precipitation and temperature. The SPEI combines the sensitivity of the Palmer Drought Severity Index (PDSI) to changes in evaporation demand (caused by temperature fluctuations and trends) with the multi-temporal nature of the Standardized Precipitation Index (SPI). Further details on the drought indicator have been provided by Vicente-Serrano et al. (2010).

The drought dataset used (the SPEIbase, which is based on SPEI) covers the entire Earth at time scales from 1 to 48 months at a spatial resolution of 0.5°, providing temporal coverage for the period 1901−2006. This dataset combines improved spatial resolution with the operative capability of previous gridded drought datasets based on the PDSI, and enables identification of various drought types. Details of the SPEIbase have been reported by Vicente-Serrano et al. (2010b) and Beguería et al. (2010). In this study we used time scales from 1 to 12 months to isolate the annual effects of the ENSO events.

Figure 2 provides an example of the evolution of the SPEI at time scales of 3, 6, 9 and 12 months in an area of central France (46.5°N, 8°E). At the shorter time scales (e.g. 3 months) there is a continuous alternation of short dry and humid periods. At these time scales drought indices are considered to represent agricultural or environmental conditions because they indicate the water content of vegetation and soils (Ji and Peters, 2003; Vicente-Serrano, 2007; Quiring and Ganesh, 2010). At longer time scales (e.g. 12 months) droughts were less frequent but lasted longer. These time scales are commonly considered representative of hydrological drought conditions, because they show the strongest correlation with river flows and reservoir storages (Szalai et al., 2000; Vicente-Serrano and López-Moreno, 2005; Lorenzo-Lacruz et al., 2010).

**2.3. Analysis**

An empirical methodology similar to that adopted by Ropelewski and Halpert (1986, 1987, 1996), Piechota and Dracup (1996) and Karabörk and Kahya (2003) was used to determine the impact of El Niño and La Niña years on global drought conditions. The approach followed that of a previous study (Vicente-Serrano, 2005) that analyzed the impact of ENSO events on droughts in the Iberian Peninsula. Average SPEI anomalies at various time scales were calculated for El Niño and La Niña years, and the year preceding.

To determine whether the SPEI at different time scales reflected significant humid or dry conditions during El Niño or La Niña phases, the Wilcoxon-Mann-Whitney test was used (Siegel and Castelan, 1988). The Wilcoxon-Mann-Whitney test is based on ranks that do not require normally distributed samples, and is slightly less powerful than parametric tests including the t-test (Helsel and Hirsch, 1992). The SPEI values in each of the months of El Niño/La Niña years were compared with the values of the SPEI for the months of normal years and those with the opposite sign. Thus, to determine the role of the El Niño years the SPEI values during La Niña years were added to the SPEI values during normal years, and vice versa. The significance level was defined as $\alpha < 0.05$.

### 2.4. Analysis of the atmospheric driving mechanisms

In order to analyze the possible physical mechanisms and atmospheric patterns that propagate the El Niño and La Niña signal on droughts worldwide we obtained the average standardized anomalies of global Sea Surface Temperature (SST), Sea Level Pressure (SLP) and 500 hPa geopotential heights corresponding to the months of El Niño and La Niña phases. For the SST, the Extended Reconstruction Sea Surface Temperature (ERSST) v3.b dataset at a resolution of 2º degrees was used (Smith and Reynolds, 2004). The SLP and 500 hPa monthly fields were obtained from the Twentieth Century Reanalysis at a resolution of 2º for the period 1901-2006 (Compo et al., 2011).

## 3. RESULTS

### 3.1 La Niña events and multi-scalar droughts globally

Figure 3 shows the monthly average anomalies of the 1-month SPEI during years under La Niña conditions, and from April of the previous year, when negative anomalies in the moisture conditions had been identified. The possible positive anomalies are not shown because the study focus was on droughts associated with ENSO events. Major negative moisture anomalies over large areas of the world were evident at the 1-month time scale from the middle of the preceding year. Thus, in June and July of the year prior to the La Niña event dry conditions were recorded in areas of South Africa, Europe and North America, but from November of the previous year to March of the La Niña year the main negative anomalies occurred on the American continent. The major anomalies detected globally occurred in the southern USA/northern Mexico region. From November to March the anomalies continuously covered large areas of this region, but even until June patchy areas with significant negative anomalies were detected during La Niña years. The effects were also evident in some regions of South America from November to January, and in parts of Eurasia.

At the time scale of 3 months the drought conditions associated with La Niña phases, which had been observed in the regions with negative anomalies at the time scale of 1 month, were confirmed and propagated over longer periods (Fig. 4). For example, in regions of South Africa significant negative anomalies were identified from June to September of the year prior to the La Niña phase. Nevertheless, the effect was most evident in southern USA/northern Mexico, where strong negative and significant anomalies in the SPEI were found for La Niña events. Negative anomalies were also found in areas of northern Argentina and southern Brazil from November in the year prior to a La Niña event to January in the event year. Moreover, in eastern Europe and western Russia negative anomalies were clearly evident from March to May of La Niña years.

At the 12-month time scale the negative SPEI anomalies were confirmed in terms of duration and magnitude (Fig. 5). It is notable that at this time scale drought conditions were identified earlier in southern Russia and Kazakhstan (from March to May) than in the southern USA/northern Mexico region, where the negative anomalies were identified from May of La Niña years and propagated to

240 the end of the year. Other areas of the world also showed negative anomalies in some months
241 (mainly in South America and some regions of east Africa). Nevertheless, the surface area affected
242 was much smaller than in the Russia/Kazakhstan and USA/Mexico regions noted above.
243
244 **3.2 El Niño events and multi-scalar droughts globally**
245 Figure 6 shows the 1-month negative SPEI anomalies corresponding to El Niño events and the
246 preceding year. The surface extent and duration of the anomalies show that large areas of the world
247 had negative anomalies lasting several months. At the time scale of 1 month the impacts were
248 evident very early in some areas. For example, the El Niño phenomenon began to cause significant
249 negative SPEI anomalies throughout most of Australia in April of the preceding year. Three months
250 later (in July) the anomalies affected most of Indonesia, the Indochina Peninsula, parts of India, the
251 majority of central America, and regions of South America. The same pattern was evident between
252 September and October, but from November of the previous year to July of the El Niño year, large
253 areas of the world showed negative SPEI anomalies. There was substantial variability across the
254 world with respect to the start and duration of droughts related to El Niño events. For example,
255 generalized negative anomalies in Australia ceased in December of the year prior to El Niño events,
256 whereas a large area in the north of South America showed negative average anomalies from
257 December to March; following this the negative anomalies were displaced over the Amazon and
258 northeast Brazil, with significant impacts on drought until August. In India the negative anomalies
259 expanded from January to June, with some major differences among months. South Africa, Canada
260 and the Sahel region also showed negative anomalies for several months from December of the
261 previous year to September of the El Niño year.
262 At the time scale of 3 months the spatial pattern of the negative SPEI anomalies was more
263 homogeneous than that observed at the 1-month time scale (Fig. 7). In Australia, generalized
264 negative anomalies occurred from May of the year prior to the El Niño year to January of the El

Niño year. Thus, the earliest impacts of El Niño events on droughts were evident in this region of the world. Similarly, in Central America strong negative 3-month SPEI averages were evident from July to October in the year prior to El Niño events. The early influence of El Niño on the occurrence of dry conditions was also apparent in Indonesia. In this area significant negative SPEI anomalies lasted until March of the El Niño years. It is notable that the cumulative properties of the SPEI allow identification of the spatial displacements of negative SPEI anomalies among regions. For example, in the western Pacific and Indian Ocean regions it was observed that dry conditions appeared in eastern Australia very early (in April of the year prior to El Niño events), and progressively affected more areas in May and June, which are the months in which the negative anomalies moved to New Guinea. From July to November of the year prior to El Niño events the strongest negative anomalies occurred in Indonesia, although some areas of India, Indochina and Australia were also affected. However, from January to June in El Niño years the negative anomalies were not evident in Australia and progressively disappeared from Indonesia, but Indochina and most of India were affected by very strong negative anomalies. In South America the impact of El Niño events on 3-month droughts was initially evident in the northernmost region from October of the year prior to El Niño events, but strong negative anomalies affecting large areas were identified from January to April of El Niño years; the anomalies subsequently moved toward the Amazon region from May to August. Also notable were the strong negative anomalies found in large areas of Canada from January to June, the very strong negative and generalized 3-month SPEI anomalies in the South Africa region from February to July, and the late impacts in the Sahel, from July to December.

It is at the time scale of 12 months where the negative SPEI anomalies reinforce the results identified at the time scale of months; clearly the effects were delayed in time (Fig. 8). Dry conditions were recorded in the western Pacific and Indian Ocean regions from September of the year prior to El Niño events to November in the El Niño year (with some spatial differences among

290 months), but in general more homogeneous patterns were found than occurred at shorter time
291 scales. The same pattern was observed in South America and South Africa, where the spatial
292 patterns were more homogeneous and stable over time than those observed at shorter time scales. In
293 contrast, other regions (e.g. Canada) where large areas were affected by negative SPEI anomalies at
294 short time scales did not show significant negative anomalies at the time scale of 12 months.
295
296 **3.3 Synthetic analysis**
297 The figures described above identify regions of the world and the months and time scales of drought
298 in which dry conditions are associated with extreme ENSO events (El Niño and La Niña). Figure 9
299 shows the regions of the world most affected by the negative anomalies of the SPEI. As the spatial
300 patterns of drought-affected regions commonly change among months, it is difficult to define
301 homogeneous regions for assessing the impact. Figure 13 shows the average SPEI anomalies of
302 representative locations in regions where El Niño or La Niña events determining drought conditions
303 were observed over a number of months and time scales. For La Niña events the regions involved
304 were northern Mexico and southern Russia, and for El Niño events the regions involved were South
305 Africa, Indonesia, eastern Australia, northern Brazil, India and the Sahel. In general, the regions
306 showed how the drought conditions are recorded from short to long time-scales for the
307 corresponding ENSO event, being more evident the effects with longer time-scales. The negative
308 anomalies were initially recorded at short time scales during the late summer or autumn of the year
309 prior to the event; exceptions included in eastern Australia, where anomalies were recorded in the
310 spring of the year preceding the event, and in the Sahel, where anomalies were recorded in summer
311 of the preceding year. During the following months the anomalies on longer time scales
312 strengthened as a consequence of the accumulation of the short-term negative anomalies. When the
313 1-month negative anomalies were recorded for different months the negative anomalies for the
314 following months were evident at both long and short SPEI time scales (e.g. Indonesia). In contrast,

315 when the 1-month anomalies were recorded over several months the negative anomalies were only
316 propagated at the longer time scales. This was evident in northern Mexico, where negative
317 anomalies at the 1-month time scale were initially evident in November of the year prior to the La
318 Niña event, whereas two months latter (in January) the 5-month time scale was the shortest for
319 which a significant negative anomaly was found.
320 The figure 9 shows that in regions affected by dry conditions during La Niña years (northern
321 Mexico and southern Russia) the period with negative anomalies was shorter and of lower
322 magnitude than occurred in regions affected by El Niño. The SPEI anomalies in South Africa,
323 eastern Australia and northern Brazil showed very strong negative magnitudes (< –1.25) over
324 several months in the El Niño year and in the preceding year, and encompassed various time scales.
325 In contrast, in northern Mexico the minimum values of the average SPEI were recorded at the 6-
326 month time scale in the year of La Niña event (SPEI = –0.95), and in southern Russia the minimum
327 value (–0.81) was recorded in May at the12-month time scale.
328 Figure 10 shows the percentage of the world where the average of the1-, 3-, 6- and 12-month SPEI
329 values were < –0.5 and < –0.8 for La Niña and El Niño events and the preceding years. Two
330 thresholds were selected to assess the effect on moderate and more severe global dry conditions. At
331 the time scale of 1 month the surface of the world with average SPEI values < –0.5 oscillated about
332 5% for both El Niño and La Niña phases, although it was observed that for most months of the
333 years in which the events occurred (from January to August) the surface area corresponding to El
334 Niño phases was much greater than for La Niña phases. The difference was more evident for the
335 surface area with SPEI values < –0.8 (corresponding to very dry conditions); the surface area
336 affected by anomalies below this threshold was lower, but the difference between the El Niño and
337 La Niña events was much clearer. The differences between El Niño and La Niña phases at the time
338 scale of 1 month were magnified at longer time scales. At the time scale of 3 months more than the
339 6% of the world showed average SPEI values < –0.5 from September of the year prior to El Niño

phases to October of the El Niño year, but for late spring and early summer (April to July) 10% of the world showed an average SPEI < –0.5. In contrast, during La Niña phases the surface area affected by droughts was much lower (< 5%). The difference was even more evident for an SPEI threshold of –0.8, because very few areas of the world were identified with La Niña phases compared with 2–3% of the world with El Niño phases. The differences were enhanced at time scales of 6 and 12 months, especially for the most severe droughts (SPEI < 0.8).

### 3.4. Related atmospheric mechanisms

Figure 11 shows the average values of the standardized 500 hPa geopotential heights corresponding to La Niña years. Large negative 500 hPa geopotential heights anomalies are recorded in the Pacific region, but also propagated throughout the intertropical zone around the globe, from November of the previous year to July of La Niña year. This could be explained further by the observed cooling of the Eastern Pacific basin, as it is shown with the large negative SST anomalies identified over most of this tropical region from August of the preceding year to May of La Niña year (see Figure S5 in the supplementary material section). In addition, there are moderate positive 500 hPa geopotential heights anomalies affecting the southern and western part of North America during the months in which the most negative SPEIs at the time scale of 1 month were recorded in this region (November, December, February and March) (see Figure 3). Also in the Eastern Europe, the pattern of dominant negative 1-month SPEI is related to positive pressure 500 hPa anomalies, light to moderate from February to May during La Niña year. The surface conditions represented by the Sea Level Pressure (SLP) anomalies could also help to explain the pattern of negative SPEI anomalies observed during La Niña phases over these regions (see Figure S6 in the supplementary material section). In any case, the magnitude of the 500 hPa geopotential heights and SLP anomalies and the general atmospheric circulations prone to cause droughts are progressively smoothed from May of

La Niña year. This would explain the very few negative SPEI anomalies at the time scale of one month recorded from May of La Niña year worldwide.

During El Niño episodes, strong positive SST anomalies in the Eastern Pacific basin are observed from June of the previous year to May of the El Niño year (see Figure S7 in the supplementary material section). These large positive SST anomalies dramatically affect the low- and mid-level atmospheric circulation during several months. In the case of El Niño, it is very clear that the effect on the 1-month negative SPEI anomalies is driven by different factors as a function of the region of the world. The early effects of the El Niño are recorded in Indonesia (from July to December of the previous year; see Figure 6) and Australia (mainly from October to December of the previous year; see Figure 6), and they are mainly driven by the strong positive SLP anomalies observed over the Western Pacific basin (Fig. 12). The colder than average SSTs in the Western Pacific region are having a clear effect on the SLP conditions, resulting in a strong anticyclonic weather pattern centered over Indonesia. This is a simultaneous effect of the El Niño on the drought conditions driven by coupled sea surface-low troposphere interactions. Nevertheless, the main effects of El Niño on droughts are propagated by means of the mid-troposphere anomalies summarized by the maps of anomalies at the 500 hPa geopotential height (see Figure 13). High pressure SLP anomalies in the Western Pacific basin between September of the previous year to April of El Niño year propagates to the mid-level troposphere between November of the previous year to June of El Niño year (particularly stronger in February-March), determining the occurrence of strong high pressure anomalies at the 500 hPa level in most of the intertropical area  Therefore, there is a clear propagation of the negative SST anomalies to the positive SLP anomalies observed in the Western Pacific basin. Consequently, these low-level anomalies are propagated throughout the entire intertropical region reinforcing anticyclonic conditions at mid-level of the troposphere 6 months after the SST anomalies in the Western Pacific region develop. Whereas for La Niña years very few land areas are affected by positive 500 hPa geopotential height anomalies, for El Niño years a large

389 emerged area shows a dominant anticyclonic circulation . For example, in the case of Australia and
390 Indochina the first strong positive 500 hPa anomalies are recorded in November and December of
391 the previous year, corresponding to strong negative 1-month SPEI anomalies over most of the
392 region. Thus, there is a high agreement between the areas with the strongest positive anomalies in
393 surface and 500 hPa pressures and the most negative SPEIs recorded each month of El Niño phase.
394 For instance, the negative 1-month SPEIs are recorded in Canada, northern part of South America,
395 South Africa, South India, and the Asian region from Indochina to the North Australia in December
396 of the previous year, wich correspond to the regions with the strongest positive anomalies at the 500
397 hPa geopotential height. From January to July of the El Niño year, negative 1-month SPEI values
398 are recorded in different regions of the world affected by positive pressure anomalies at the mid-
399 troposphere, which are very persistent in areas like South Africa and South India where the negative
400 1-month SPEI values are recorded in most of the months from February to July of El Niño year.
401 The results show that although the patterns of anomalies of SST, SLP and 500 hPa heights are
402 persistent for different months of El Niño and La Niña phases, the influence on the areas in which
403 the ENSO phenomenon is determining drought conditions is restricted to few months at the time
404 scale of 1 month. Therefore, the delays in the drought onset at longer time scales (e.g. 6- or 12-
405 months) occur due to a delay in the local hydrological response and are not associated with the
406 atmospheric circulation response to the SST anomalies or the evolution of the SST anomaly itself.
407 As a result, the anomalies recorded at longer time-scales, representative of different types of
408 drought, will be caused by the cumulative dry conditions in some specific months, commonly
409 coeval with the strongest ENSO signal in the SST and atmospheric circulation anomalies. These
410 anomalies will then propagate throughout the hydrological cycle to cause droughts at long time-
411 scales. Nevertheless, for El Niño phases, the persistence of the 1-month SPEI anomalies is
412 commonly stronger than that found for La Niña phases (e.g., in the northern South America and

South Africa), explaining that droughts are propagated at longer SPEI time-scales several months after finishing the SST and related atmospheric circulation anomalies.

## 4. DISCUSSION AND CONCLUSIONS

We presented here the first global analysis of the ENSO impact on multi-scalar droughts, focusing on the effects of the warm (El Niño) and cold (La Niña) events of the ENSO phenomenon. The results showed that very dry conditions occurred during both phases in different areas of the world. Thus, the spatial extent and the months in which the impacts were recorded varied significantly during the events. The impact of warm and cold phases of the ENSO have been analyzed and described in previous global studies (Kouski et al., 1984; Ropelewski and Halpert, 1987 and 1996; Halpert and Ropelewski, 1992; Kiladis and Díaz, 1989; Díaz et al., 2001; Dai et al., 2004; Sheffield et al., 2009; Appipatanavis et al., 2009), and in several regional and local studies focused on particularly sensitive regions (e.g. Harger, 1995; Chiew et al., 1998; Bonsal and Lawford, 1999; Richard et al., 2001; Karnauskas et al., 2008; Villar et al., 2009; Kothawale, 2010). Although our results are consistent in general terms with previous findings, we have provided strong evidence that the magnitude of the drought conditions recorded in each region shows large variations as a function of the drought time scale. Thus, the results showed that the period in which dry conditions were identified in each affected region tended to increase by some months as the time scale became longer. This resulted from the procedure for calculation of the multi-scalar drought index, because longer time scales generated smoother fluctuations and thus a larger sequence of anomalies with the same sign. The main implication of the results is the potential to improve assessment of the possible agricultural, environmental, hydrological and economic impacts, based on the ability of the different drought time scales to represent the temporal variability of various usable water sources.

Nevertheless, it is noteworthy that both the timing of the impacts and the spatial pattern of negative SPEI anomalies for both the warm and cold phases varied as a function of the time scale. At short

time scales the main regions affected by negative SPEI anomalies were clearly identified. However, they showed some variability, with large differences in the spatial patterns and the magnitude of the anomalies among the months of the event. Thus, at short time scales the negative anomalies that were identified showed a very patchy pattern, which was more evident during La Niña events. In contrast, at longer time scales the spatial pattern of negative anomalies was more coherent; fewer but larger regions were affected, and the temporal variability in the affected areas and the magnitude of the anomalies was low. Thus, longer time scales emphasized the ENSO effects and clearly distinguished regions where the expected influence of the ENSO phases was uncertain or statistically significant. At short time scales sustained negative anomalies during most ENSO phases will produce marked dry conditions at longer time scales. In contrast, the influence on droughts is smoothed at longer time scales in those regions only affected over a few months, or where the events exhibit negative anomalies. As mentioned above, this will have significant consequences for those hydrological subsystems with long response times to dry climate conditions, such as ground water reserves and large reservoirs (e.g. Peters et al., 2005; Lorenzo-Lacruz et al., 2010).

This study highlighted a number of regions that are markedly affected by drought at a wide range of time scales in response to El Niño and La Niña phases. Those regions affected by La Niña phases were southern USA/northern Mexico and southern Russia/eastern Europe, whereas for El Niño phases the most affected areas were South Africa, Indonesia and the western Pacific area, Australia, the northern part of South America and the Amazon, India and the Indochina peninsulas, central and western Canada, and large areas of the Sahel. These results agree with the impact of positive and negative ENSO phases on global precipitation. For example, Ropelewski and Halpert (1987) showed in the West Pacific region and El Niño phases low precipitation during most of the months of the year. In India the negative precipitation anomalies are found between June and September of the previous year to El Niño and in South Africa between July of the previous year and March of El

Niño years, a similar pattern that found in northeastern South America. Thus, we found negative SPEI anomalies for most of these months and regions by means of a SPEI 1-month time-scale. Ropelewski and Halpert (1989) also analyzed La Niña phases, showing a smaller number of anomalies associated with La Niña phases in relation to those identified for El Niño. Nevertheless, these previous global studies showed very low monthly precipitation anomalies for most of the regions and the areas in which the main effect of La Niña phases on droughts have been identified here (e.g., South North America) are not so clearly identified analyzing monthly precipitation anomalies. The droughts associated with La Niña phases in Southern USA and Northern Mexico were described by Kahya and Dracup (1994), which detected negative streamflow anomalies appearing at the beginning of La Nina event year until October of the same year. In any case, at the time-scale of 1 month the magnitude of the negative SPEI anomalies found worldwide are, in general, low and comparable to the magnitude observed by the studies cited above using monthly precipitation. Thus, we clearly observe that when the cumulative effects summarized by longer SPEI time-scales are analyzed larger anomalies are identified.

We have also analyzed the Sea Surface Temperature and the atmospheric circulation patterns that the ENSO signal propagates on droughts worldwide. Although the dynamic of the El Niño and La Niña phases had been widely analysed (e.g., Rasmusson and Carpenter, 1982; Clarke, 2008 and references therein) and also their connection with the surface climate (e.g., Gershunov and Barnett, 1998; Allan et al., 1996), we have illustrated here the high relationship between atmospheric circulation anomalies and the SPEI averages in those regions in which El Niño or La Niña phases are prone to cause droughts. The effect of the ENSO phases on droughts is mainly propagated throughout the mid-trophosphere (Enfield and Mestas-Núñez, 1999; Mo, 2000), with a delay of some months regarding the SLP anomalies in the Western Pacific area as a consequence of the colder than average SST anomalies. The effect of the anomalies in the atmospheric circulation on dry conditions are detected for several months of each one of the ENSO phases, but mainly for El

Niño years in which persistent negative SPEIs at the time scale of 1-month are recorded in some regions (e.g., South Africa or India). Nevertheless, the propagation of the drought conditions at longer time-scales (e.g., 6- or 12-months) is not directly determined by the atmospheric circulation response to the SST anomalies, since the SPEI anomalies will be caused by the cumulative dry conditions in some specific months, which may propagate several months after the SST *or the atmospheric circulation anomalies associated with the ENSO phases disappear.*

The number of regions and months affected and the total surface area with negative anomalies was much higher for El Niño events than for La Niña events. In summary, El Niño events tended to generate more droughts globally than La Niña events. This is in agreement with the recent findings of Sheffield et al. (2009), who showed that there is a tendency for more short-term drought events to occur during El Niño phases. Nevertheless, our results show that the tendency to more regions and stronger negative anomalies for El Niño events relative to La Niña events clearly increases with an increase in the time scale over which the drought is quantified. Thus, at the longest time scales the percentage of the global surface area affected by drought during El Niño years was more than four times that for La Niña years. This implies that El Niño events affect more regions and have greater impact, but also that the associated dry conditions are more persistent over time. Smith and Ropelewski (1997) concluded that (i) in several regions where the ENSO influence has been identified, the impact is greater for one phase (El Niño or La Niña) than the other, and (ii) in general, the influence on precipitation at the global scale is greater during La Niña events than during El Niño events, which is a pattern that has also been observed for soil moisture modeled at the global scale (Sheffield et al., 2009). This result is expected because during El Niño events tropical precipitation shifts to the central Pacific Ocean and away from tropical land areas. Thus, during El Niño phases tropical land masses dry while wet over land is restricted to southern North America and a small part of southern South America. The opposite is true during La Nina events.

Our results also showed differences in the timing of the influence of ENSO events in different regions of the world, independent of the drought time scale. The ENSO effect typically has a temporal delay, which is longer where more remote is the connection (Kiladis and Díaz, 1989; Stone et al., 1996). The lags in impact are very complex when quantified at various time scales. Nevertheless, in the most affected regions of the world we did not find early effects (at the beginning of the corresponding ENSO events) during La Niña phases, whereas for El Niño phases early effects were clearly evident in areas including Australia and Indonesia. Moreover, the effects of El Niño phases lasted for many months, and in some regions (e.g. the Sahel) the impact of El Niño on droughts could be detected more than one year after the beginning of the warm phase.

It is notable that the effect of ENSO events on droughts clearly lagged in different regions of the world, and that there was spatial displacement of the affected areas to neighboring regions as the ENSO event developed: the most obvious case was the displacement of drought conditions towards Indonesia from Australia at the beginning of El Niño events, followed by advance to the Indochina peninsula and finally to India.

Lags in the impacts of ENSO events and their propagation to neighboring areas offer a unique mechanism for drought prediction. The development of measures for drought planning and preparedness is a priority in reducing drought hazards (Wilhite, 1996; Wilhite et al., 2007; Prabhakar and Shaw, 2008). A critical component in drought planning is the provision of timely and reliable climate information on which to base management decisions (Svoboda et al., 2004). Hence, drought monitoring is crucial for the implementation of drought plans and the use of synthetic drought indicators, including the SPEI used in this study. Such indicators can provide accurate information about the spatial extent and severity of drought conditions in a way that reflects the level of risk in real time.

The capacity to accurately predict droughts prior to their onset would markedly improve the management of risk, and reduce its associated impacts. However, relative to drought monitoring the

539 forecasting of droughts is still unreliable. The unique system for drought forecasting in the USA is
540 based on a combination of sources including the Constructed Analogue on Soil moisture, the
541 Climate Forecast System seasonal precipitation forecasts, the El Niño precipitation and temperature
542 composites for November–January, normal climatology, and the current drought conditions
543 (Schubert et al., 2007). Recent studies in Europe have indicated the possibility of providing
544 seasonal anomaly forecasts, using the influence of driving factors including the ENSO phase (Frias
545 et al., 2010).
546 The prediction of ENSO events has increased with the refinement of numerical models (Chen et al.,
547 2004; Tippet and Barnston, 2008; Jin et al., 2008). However, we have shown that prediction of
548 drought impacts related to ENSO can be possible too based only on observations, because there is
549 commonly a delay of some months from the onset of ENSO events (typically in April–May of the
550 previous year) to the occurrence of drought. The prediction can be even more robust for those water
551 sources related to long drought time scales (e.g. ground water and reservoir storages), where the
552 delay is even longer. In regions such as Australia, where the ENSO impact on droughts are
553 identified very early (at the beginning of the ENSO phases), the potential to predict is very limited
554 and dependent on numerical prediction of the occurrence of ENSO events. Nevertheless, given the
555 large temporal lag between the development of ENSO phenomena and the identification of drought
556 conditions, it appears possible to detect in advance the likely impact of the ENSO on drought in the
557 majority of regions, at time scales comparable to those in this study.
558 Although some studies have found a nonstationary relationship between the surface climate and the
559 ENSO variability in some regions (e.g. Lloyd-Hughes and Saunders, 2002; Kane, 2006), recent
560 analyses have demonstrated that the linear ENSO teleconnections are stable and robust, and there is
561 no evidence that changes in the strength of the teleconnections between ENSO and the atmospheric
562 circulation went beyond chance in the recent past (Sterl et al., 2007). Established relationships

between ENSO phases and drought indices therefore seem appropriate for drought prediction over large areas of the world.


## ACKNOWLEDGEMENTS

This work has been supported by the research projects CGL2008-01189/BTE and CGL2006-11619/HID financed by the Spanish Commission of Science and Technology and FEDER, EUROGEOSS (FP7-ENV-2008-1-226487) and ACQWA (FP7-ENV-2007-1- 212250) financed by the VII Framework Programme of the European Commission, "Las sequías climáticas en la cuenca del Ebro y su respuesta hidrológica" and "La nieve en el Pirineo aragonés: Distribución espacial y su respuesta a las condiciones climáticas" Financed by "Obra Social La Caixa" and the Aragón Government.


## REFERENCES


Allan, R., Lindesay, J., and Parker, D., (1996): *El Nino Southern Oscillation and climatic variability*. CSIRO, 416 pp. Australia.

An, S.I., and Jin, F.F., (2004): Nonlinearity and asymmetry of ENSO. *Journal of Climate* 17: 2399–2412.

Apipattanavis, S., McCabe, G.J., Rajagopalan, B. and Gangopadhyay, S. (2009): Joint Spatiotemporal Variability of Global Sea Surface Temperatures and Global Palmer Drought Severity Index Values. *Journal of Climate* 22: 6251-6267.

Balling Jr., R.C., Goodrich, G.B., (2007): Analysis of drought determinants for the Colorado River Basin. *Climatic Change*, 82: 179-194.

Beguería, S., Vicente-Serrano, S.M. and Angulo, M., (2010): A multi-scalar global drought data set: the SPEIbase: A new gridded product for the analysis of drought variability and impacts. *Bulletin of the American Meteorological Society*. DOI: 10.1175/2010BAMS2988.1

Bonsal, B.R. and Lawford, R.G., (1999): Teleconnections between el niño and la niña events and summer extended dry spells on the Canadian prairies. International *Journal of Climatology* 19: 1445–1458.

Breshears, D.D., Cobb, N.S., Rich, P.M., et al., (2005): Regional vegetation die-off in response to global-change-type drought. *PNAS* 102: 15144-15148.

Brönnimann, S., Luterbacher, J., Staehelin, J., Svendby, T.M., Hansen G. and Svenøe, T. (2004): Extreme climate of the global troposphere and stratosphere in 1940-42 related to El Niño. *Nature* 431: 971-974.

Brönnimann, S., (2007): Impact of El Niño–Southern Oscillation on European climate. Reviews of Geophysics 45. doi:10.1029/2006RG000199

Brown, J.N., McIntosh, P.C., Pook, M.J. and Risbey, J.S., (2009): An investigation of the links between ENSO flavors and rainfall processes in Southeastern Australia. *Monthly Weather Review* 137: 3786-3795.

603 Chen, D., Cane, M. A., Kaplan, A., Zebiak, S.E. and Huang, D.J., (2004): Predictability of El Nino
604 over the past 148 years, *Nature* 428, 733– 736.
605 Chiew, F.H.S., Piechota, T.C., Dracup, J.A., and McMahon, T.A., (1998): E1 Nino/Southern
606 Oscillation and Australian rainfall, streamflow and drought: Links and potential for
607 forecasting. *Journal of Hydrology* 204: 138 149.
608 Ciais, Ph., Reichstein, M., Viovy, N., et al., (2005): Europe-wide reduction in primary productivity
609 caused by the heat and drought in 2003. *Nature* 437: 529-533.
610 Clarke, A., (2008): An Introduction to the Dynamics of El Nino & the Southern Oscillation.
611 Academic Press. 324 Pages
612 Compo, G.P., Whitaker, J.S., Sardeshmukh, P.D., Matsui, N., Allan, R.J., Yin, X., Gleason, B.E.,
613 (...), Worley, S.J., (2011): The Twentieth Century Reanalysis Project. *Quarterly Journal of*
614 *the Royal Meteorological Society*, 137: 1-28
615 Cordery, I. and McCall, M., (2000): A model for forecasting drought from teleconections. *Water*
616 *Resources Research*, 36: 763-768.
617 Dai, A., Trenberth, K.E. and Qian, T., (2004). A Global Dataset of Palmer Drought Severity Index
618 for 1870–2002: Relationship with Soil Moisture and Effects of Surface Warming. *Journal of*
619 *Hydrometeorology* 5: 1117-1130.
620 D'Arrigo, R. and Wilson, R., (2008): El Niño and Indian Ocean influences on Indonesian drought:
621 Implications for forecasting rainfall and crop productivity. *International Journal of*
622 *Climatology*, 28: 611-616.
623 Díaz, H.F. and Kiladis, G.N., (1992): Atmospheric teleconnections associated with the extreme
624 phases of the Southern oscillation. En El Niño: Historical and paleoclimatic aspects of the
625 Southern oscillation (H.F. Díaz y Markgraf V. Eds.). Cambridge University Press: 7-28.
626 Enfield, D.B. and Mestas-Nuñez, A.M., (1999): Multiscale variabilities in global sea surface
627 temperatures and their relationships with tropospheric climate patterns. *Journal of Climate*,
628 12: 2719-2733
629 Fowler, A. and Adams, K., (2004) Twentieth century droughts and wet periods in Auckland (New
630 Zealand) and their relationship to ENSO. *International Journal of Climatology* 24: 1947-
631 1961.
632 Frías M.D., S. Herrera, A.S. Cofiño, J.M. Gutiérrez (2010) Assessing the Skill of Precipitation and
633 Temperature Seasonal Forecasts in Spain. Windows of Opportunity Related to ENSO
634 Events. *Journal of Climate* 23: 209-220.
635 Gershunov, A. and Barnett, T.P., (1998): Interdecadal Modulation of ENSO Teleconnections.
636 *Bulletin of the American Meteorological Society*, 79: 2715-2725.
637 Halpert, M.S. and Ropelewski, C.F., (1992): Surface temperature patterns associated with the
638 Southern oscillation. *Journal of Climate*, 5: 577-593.
639 Hannachi, A., Stephenson, D. B. and Sperber, K.R., (2003): Probability-based methods for
640 quantifying nonlinearity in the ENSO. *Climate Dynamics*, 20: 241–256.
641 Harger, J.R.E., (1995): ENSO variations and drought occurrence in Indonesia and Philippines,
642 Atmospheric Environment 29: 1943-1955.
643 Helsel, D. R., and Hirsch, R. M., (1992): Statistical Methods in Water Resources, 522 pp., Elsevier,
644 New York.
645 Hendon, H.H., (2003): Indonesian rainfall variability: Impacts of ENSO and local air-sea
646 interaction. *Journal of Climate*, 16: 1775-1790.
647 Hoerling, M.P., Kumar, A. and Zhong, M., (1997): El Niño, La Niña, and the Nonlinearity of Their
648 Teleconnections. *Journal of Climate* 10: 1769-1786.
649 Janicot, S., Moron, V. and Fontaine, B., (1996): Sahel droughts and ENSO dynamics. *Geophysical*
650 *Research Letters* 23: 515-518.
651 Janicot, S., Trzaska, S. and Poccard, I., (2001): Summer Sahel-ENSO teleconnection and decadal
652 time scale SST variations. *Climate Dynamics* 18: 303-320.

Ji, L. and Peters, A.J., (2003): Assessing vegetation response to drought in the northern Great Plains using vegetation and drought indices. *Remote Sensing of Environment* 87: 85-98.

Jin, E.K., Kinter III, J.L., Wang, B., et al., (2008): Current status of ENSO prediction skill in coupled ocean-atmosphere models. *Climate Dynamics* 31: 647-664.

Kane, R.P., (2006): Unstable ENSO relationship with Indian regional rainfall. *International Journal of Climatology* 26: 771-783.

Kahya, E., and J. A. Dracup (1994), The influences of type I El Niño and La Niña events on streamflows in the Pacific southwest of the United States, *J. Clim.*, 7, 965– 976.Karabörk, M.C. and Kahya, E., (2003): The teleconnections between the extreme phases of the Southern Oscillation and precipitation patterns over Turkey, *International Journal of Climatology*, 23: 1607–1625.

Karabörk, M.C¸ Kahya, E. and Karaca, M., (2005): The influences of the Southern Oscillation and North Atlantic Oscillation on hydrometeorological surface parameters in Turkey, *Hydrological Processes* 19: 1185-1211.

Karabörk, M.C. and Kahya, E., (2009): Links between the categorised Southern Oscillation indicators and climate and hydrologic variables in Turkey. *Hydrological Processes* 23: 1927-1936.

Karnauskas, K.B., Ruiz-Barradas, A., Nigam, S. and Busalacchi, A.J., (2008): North American droughts in ERA-40 global and NCEP North American Regional Reanalyses: A Palmer drought severity index perspective. *Journal of Climate* 21: 2102-2123.

Khan, S., Gabriel, H.F. and Rana, T., (2008): Standard precipitation index to track drought and assess impact of rainfall on watertables in irrigation areas. *Irrigation and Drainage Systems* 22: 159-177.

Kiladis, G.N. and Díaz, H.F., (1989): Global climatic anomalies associated with extremes in the Southern Oscillation. *Journal of Climate*, 2: 1069-1090.

Kothawale, D.R., Munot, A.A., Kumar, K.K., (2010): Surface air temperature variability over India during 1901-2007, and its association with ENSO. *Climate Research* 42: 89-104.

Kousky, V.E., Kagano, M.T., Iracema; S, and Cavalcanti, F.A., (1984): A review of the Southern Oscillation: oceanic-atmospheric circulation changes and related rainfall anomalies. Tellus A 36A: 490–504.

Lloyd-Hughes, B. y Saunders, M.A., (2002): Seasonal prediction of european spring precipitation from El Niño-southern oscillation and local sea-surface temperatures. *International Journal of Climatology*. 22: 1-14.

López-Moreno, J.I. and Vicente-Serrano, S.M., (2008): Extreme phases of the wintertime North Atlantic Oscillation and drought occurrence over Europe: a multi-temporal-scale approach. *Journal of Climate* 21, 1220-1243.

Lorenzo-Lacruz, J., Vicente-Serrano, S.M., López-Moreno, J.I., Beguería, S., García-Ruiz, J.M. and Cuadrat, J.M., (2010): The impact of droughts and water management on various hydrological systems in the headwaters of the Tagus River (central Spain). *Journal of Hydrology*, 386: 13-26.

Meehl, G.A., Karl, T., Easterling, D.R., Changnon, S., *et al.*, (2000): An introduction to trends in extreme weather and climate events: observations, socioeconomic impacts, terrestrial ecological impacts, and model projections. *Bulletin of the American Meteorological Society*. 81: 413-416.

McKee, T.B.N., J. Doesken, and J. Kleist, 1993: The relationship of drought frecuency and duration to time scales. Eight Conf. On Applied Climatology. Anaheim, CA, Amer. Meteor. Soc. 179-184.

Mo, K.C. , (2000): Relationships between low-frequency variability in the Southern Hemisphere and sea surface temperature anomalies. *Journal of Climate* 13: 3599-3610.

Mo, K.C. and Schemm, J.E., (2008) Relationships between ENSO and drought over the southeastern United States. Geophysical Research Letters 35: L15701.

Mo, K.C., Schemm, J.E., Yoo, S.-H., (2009): Influence of ENSO and the atlantic multidecadal oscillation on drought over the United States. *Journal of Climate* 22: 5962-5982.

Monahan, A. H., and Dai, A., (2004): The spatial and temporal structure of ENSO nonlinearity. *Journal of Climate* 17: 3026–3036.

Nazemosadat, M.J. and Ghasemi, A.R., (2004): Quantifying the ENSO-related shifts in the intensity and probability of drought and wet periods in Iran. *Journal of Climate* 17: 4005-4018.

Nel, W., (2009): Rainfall trends in the KwaZulu-Natal Drakensberg region of South Africa during the twentieth century. *International Journal of Climatology*, 29: 1634-1641.

New, M., Todd, M., Hulme, M. and Jones, P., (2001): Precipitation measurements and trends in the twentieth century. *International Journal of Climatology.* 21: 1899-1922.

Nicholson, S.E., (2001): Climatic and environmental change in Africa during the last two centuries. *Climate Research* 17: 123-144.

Obasi, G.O.P., (1994): WMO`s role in the international decade for natural disaster reduction. *Bulletin of the American Meteorological Society.* 75: 1655-1661.

Patel, N.R., Chopra, P. and Dadhwal, V.K., (2007): Analyzing spatial patterns of meteorological drought using standardized precipitation index. *Meteorological Applications*, 14**:** 329-336.

Peters, E., van Lanen, H. A. J., Torfs, P. J. J. F., and Bier, G., (2005): Drought in groundwater-drought distribution and performance indicators, *Journal of Hydrology* 306: 302–317.

Philander, S. G., (1990): El Niño, La Niña and the Southern Oscillation, Elsevier, New York.

Philander, S.G. and Fedorov, A., (2003): Is El Niño sporadic or cyclic?. *Annual Review of Earth and Planetary Sciences.* 31: 579-594.

Philip, S.Y. and van Oldenborgh, G.J., (2009): Significant atmospheric nonlinearities in the ENSO cycle. *Journal of Climate* 22: 4014-4028.

Piechota, T. C., and Dracup, J.A., (1996): Drought and regional hydrologic variation in the United States: Associations with the El Niño – Southern Oscillation. *Water Resources Research* 32: 1359-1373.

Prabhakar, S.V.R.K. and Shaw, R., (2008): Climate change adaptation implications for drought risk mitigation: A perspective for India. *Climatic Change*, 88: 113-130.

Quiring, S.M. and Ganesh, S., (2010): Evaluating the utility of the Vegetation Condition Index (VCI) for monitoring meteorological drought in Texas. *Agricultural and Forest Meteorology* 150: 330-339.

Rajagopalan, B., Cook, E., Lall, V. and Ray, B.K., (2000): Spatiotemporal variability of ENSO and SST teleconnections to summer drought over the United States during the Twentieth Century. *Journal of Climate*, 13: 4244-4255.

Rasmusson, E.M and Carpenter, T.M., (1982): Variations in tropical sea surface temperature and surface wind fields associated with the Southern Oscillation/El Niño. *Monthly Weather Review.* 110: 354-384.

Rayner, N. A.; Parker, D. E.; Horton, E. B.; Folland, C. K.; Alexander, L. V.; Rowell, D. P.; Kent, E. C.; Kaplan, A. (2003) Global analyses of sea surface temperature, sea ice, and night marine air temperature since the late nineteenth century J. Geophys. Res.Vol. 108, No. D14, 4407 10.1029/2002JD002670.

Redmond, K.T. and Koch, R.W., (1991): Surface climate and streamflow variability in the Western United States and their relationship to large-scale circulation indices. *Water Resources Research.* 27: 2381-2399.

Richard, Y., Fauchereau, N., Poccard, I., Rouault, M. and Trzaska, S., (2001): 20th century droughts in southern Africa: spatial and temporal variability, teleconnections with oceanic and atmospheric conditions. *International Journal of Climatology* 21: 873–885.

751 Ropelewski, C.F. and Halpert, M.S., (1986): North American precipitation and temperature patterns
752 associated with the El Niño/Southern Oscillation (ENSO). *Monthly Weather Review*. 114:
753 2352-2362.
754 Ropelewski, C.F. and Halpert, M.S., (1987): Global and regional scale precipitation patterns
755 associated with the El Niño/Southern Oscillation. *Monthly Weather Review*. 115: 1606-
756 1626.
757 Ropelewski, C.F. and Halpert, M.S., (1989): Precipitation patterns associated with the high index
758 phase of the Southern Oscillation. Journal of Climate 2: 268-284
759 Ropelewski, C. F., and Halpert, M. S., (1996): Quantifying Southern Oscillation-precipitation
760 relationships, *Journal of Climate* 9: 1043–1059.
761 Rouault, M. and Richard, Y., (2005): Intensity and spatial extent of droughts in southern Africa.
762 *Geophysical Research Letters* 32: art. no. L15702.
763 Sardeshmukh PD, Compo GP, and Penland C., (2000): Changes of probability associated with El
764 Niño. *Journal of Climate* 13: 4268–4286.
765 Schonher, T. and Nicholson, S.E., (1989): The relationship between California rainfall and ENSO
766 events. *Journal of Climate*, 2: 1258-1268.
767 Schubert, S., Koster, R., Hoerling, M., Seager, R., Lettenmaier, D., Kumar, A. and Gutzler, D.
768 (2007): Predicting drought on seasonal-to-decadal time scales. *Bulletin of the American*
769 *Meteorological Society*, 88: 1625-1630.
770 Shabbar, A. and Skinner, W., (2004): Summer drought patterns in Canada and the relationship to
771 global sea surface temperatures. *Journal of Climate* 17: 2866-2880.
772 Sheffield, J., Andreadis, K.M., Wood, E.F. and Lettenmaier, D.P., (2009): Global and continental
773 drought in the second half of the twentieth century: severity-area-duration analysis and
774 temporal variability of large-scale events. *Journal of Climate* 22: 1962-1981.
775 Siegel, S., and Castelan, N. J. (1988): *Nonparametric Statistics for the Behavioral Sciences*,
776 McGraw-Hill, New York.
777 Smith, T.M. and Ropelewski, C.F., (1997): Quantifying Southern Oscillation-Precipitation
778 relationships on atmospheric GCM. *Journal of Climate*, 10: 2277-2284.
779 Smith, T.M., and R.W. Reynolds, (2004): Improved Extended Reconstruction of SST (1854-1997).
780 *Journal of Climate*, 17, 2466-2477.
781 Sterl, A., van Oldenborgh, G.J., Hazeleger, W. and Burgers, G., (2007): On the robustness of ENSO
782 teleconnections. Climate Dynamics 29: 469-485.
783 Stone, R.C., Hammer, G.L. and Marcussen, T., (1996): Prediction of global rainfall probabilities
784 using phases of the Southern Oscillation Index. Nature 384: 252-255.
785 Svoboda, M. et al., (2002): The drought monitor. *Bulletin of the American Meteorological Society*,
786 83: 1181-1190.
787 Svoboda, M.D., Hayes, M.J., Wilhite, D.A. and Tadesse, T., (2004): Recent advances in drought
788 monitoring. *Bulletin of the American Meteorological Society*, 5237-5240.
789 Szalai, S., Szinell, C. S. and Zoboki, J., (2000): Drought monitoring in Hungary, in Early Warning
790 Systems for Drought Preparedness and Drought Management, pp. 182– 199, World
791 Meteorol. Organ., Geneva, Switzerland.
792 Tippett, M.K. and Barnston, A.G., (2008): Skill of multimodel ENSO probability forecasts.
793 *Monthly Weather Review* 136: 3933-3946.
794 Trenberth, K.E. and Guillemot, Ch.J., (1996): Physical processes involved in the 1988 drought and
795 1993 floods in north America. *Journal of Climate.* 9: 1288-1298.
796 Trenberth, K. E., and Hoar, T.J., (1996): The 1990–1995 El Niño‐Southern Oscillation Event:
797 Longest on Record. *Geophysical Research Letters*, 23: 57–60.
798 Trenberth, K.E., (1997): The definition of El Niño. Bulletin of the American Meteorological
799 Society. 78: 2771-2777.

UN, (2008): Trends in sustainable development. Agriculture, rural development, land, desertification and drought. Department of Economic and Social Affairs. United Nations. New York.

Vicente-Serrano, S.M., (2005): El Niño and La Niña influence on drought conditions at different time scales in the Iberian Peninsula. *Water Resources Research* 41, W12415, doi:10.1029/2004WR003908

VicenteSerrano, S.M. and López-Moreno, J.I., (2005): Hydrological response to different time scales of climatological drought: an evaluation of the standardized precipitation index in a mountainous Mediterranean basin. *Hydrology and Earth System Sciences* 9: 523-533.

Vicente-Serrano, S.M. (2007): Evaluating The Impact Of Drought Using Remote Sensing In A Mediterranean, Semi-Arid Region, *Natural Hazards*, 40: 173-208.

Vicente-Serrano S.M., Beguería, S. and López-Moreno, J.I., (2010): A Multi-scalar drought index sensitive to global warming: The Standardized Precipitation Evapotranspiration Index – SPEI. *Journal of Climate* 23: 1696-1718.

Vicente-Serrano, S.M., Beguería, S., López-Moreno, J.I., Angulo, M., El Kenawy, A. (2010b): A new global 0.5° gridded dataset (1901-2006) of a multiscalar drought index: comparison with current drought index datasets based on the Palmer Drought Severity Index. *Journal of Hydrometeorology*. 11: 1033–1043

Villar, J.C.E., Ronchail, J., Guyot, J.L., Cochonneau, G., Naziano, F., Lavado, W., de Oliveira, E., et al., (2009): Spatio-temporal rainfall variability in the Amazon basin countries (Brazil, Peru, Bolivia, Colombia, and Ecuador). *International Journal of Climatology* 29: 1574-1594.

Wilhite, D.A., (1996): A methodology for drought preparedness. *Natural Hazards.* 13: 229-252.

Wilhite, D.A., Svoboda, M.D. and Hayes, M.J., (2007): Understanding the complex impacts of drought: A key to enhancing drought mitigation and preparedness. Water Resources Management 21: 763-774.

# FIGURE CAPTIONS

Figure 1. Monthly SST anomalies (in degrees) corresponding to the phases of the winter El Niño (squares) and La Niña (circles). The monthly means were computed for each time series for the period 1971-2000. These means were then subtracted from their respective time series for the entire data set (1901-2006).

Figure 2. Evolution of the 3-, 6-, 9- and 12-month SPEI in central France (46.5°N, 8°E).

Figure 3. Spatial distribution of the average 1-month SPEI anomalies during La Niña years and the years preceding. The black lines identify areas in which significant differences in the SPEI average were found between the La Niña years and other years.

Figure 4. Spatial distribution of the average 3-month SPEI anomalies during La Niña years and the years preceding. The black lines identify areas in which significant differences in the SPEI average were found between the La Niña years and other years.

Figure 5. Spatial distribution of the average 12-month SPEI anomalies during La Niña years and the years preceding. The black lines identify areas in which significant differences in the SPEI average were found between the La Niña years and other years.

Figure 6. Spatial distribution of the average 1-month SPEI anomalies during El Niño years and the years preceding. The black lines identify areas in which significant differences in the SPEI average were found between the El Niño years and other years.

Figure 7. Spatial distribution of the average 3-month SPEI anomalies during El Niño years and the years preceding. The black lines identify areas in which significant differences in the SPEI average were found between the El Niño years and other years.

Figure 8. Spatial distribution of the average 12-month SPEI anomalies during El Niño years and the years preceding. The black lines identify areas in which significant differences in the SPEI average were found between the El Niño years and other years.

Figure 9. Average SPEI values at the time scales of 1–12 months in eight representative regions of the world during the ENSO phases that drive drought conditions in each region: i) La Niña (northern Mexico and southern Russia), and ii) El Niño (South Africa, Indonesia, eastern Australia, northern Brazil, India and the Sahel). The black lines identify months and time scales when significant differences in the SPEI averages were found between the corresponding ENSO phase and the remaining years

Figure 10. Percentage of the world surface where the average 1-, 3-, 6- and 12-month SPEI values were $< -0.5$ and $< -0.8$ for La Niña (black bars) and El Niño (gray bars) years and the year preceding each.

Figure 11. 500 hPa standardized anomalies during La Niña years and the years preceding.

Figure 12. SLP standardized anomalies during El Niño years and the years preceding.

Figure 13. 500 hPa standardized anomalies during El Niño years and the years preceding.

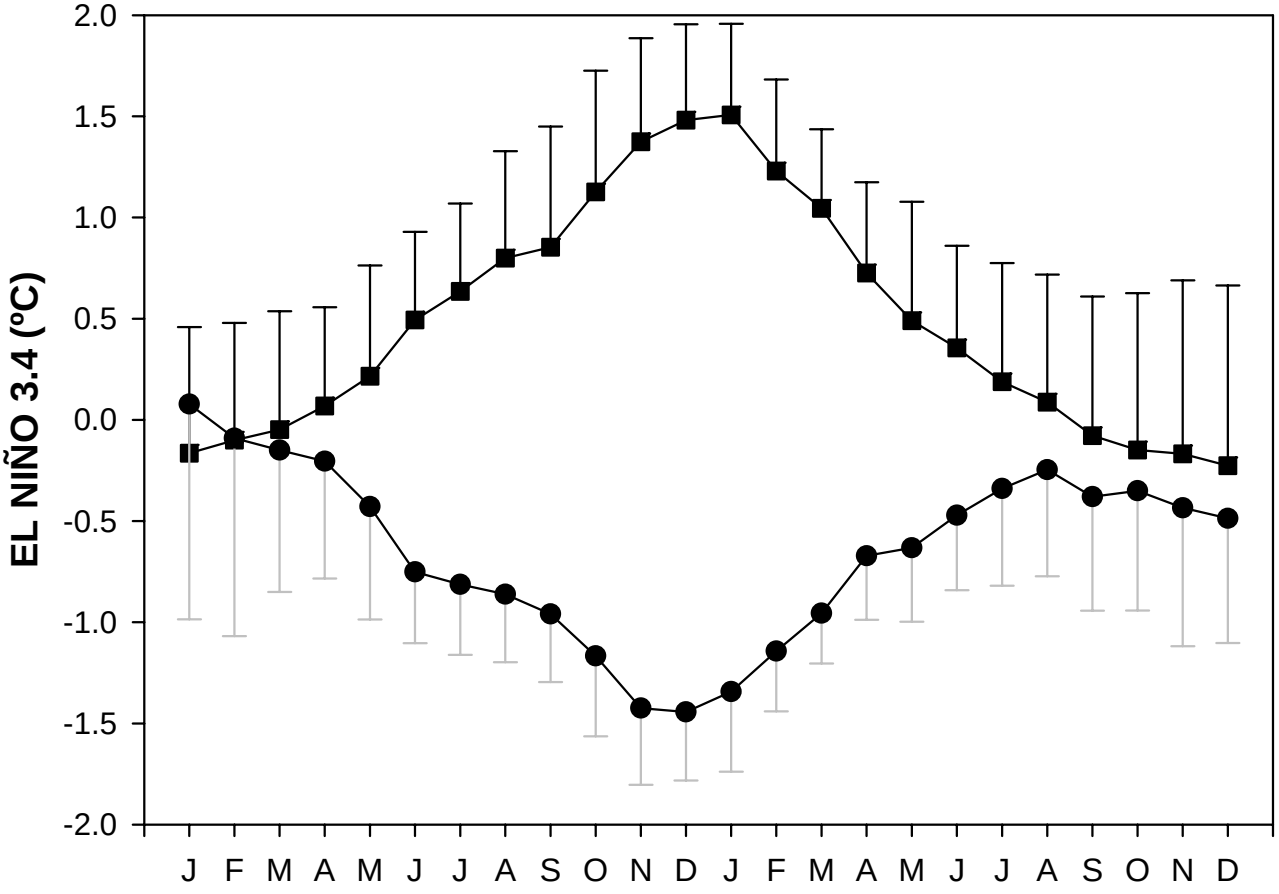


866

867 Figure 1.

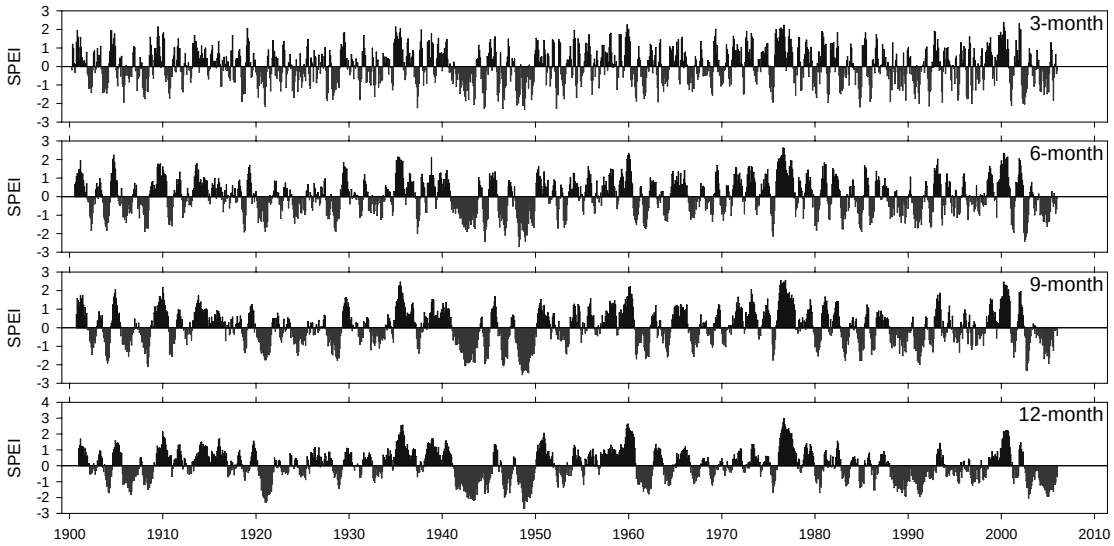


868

869 Figure 2

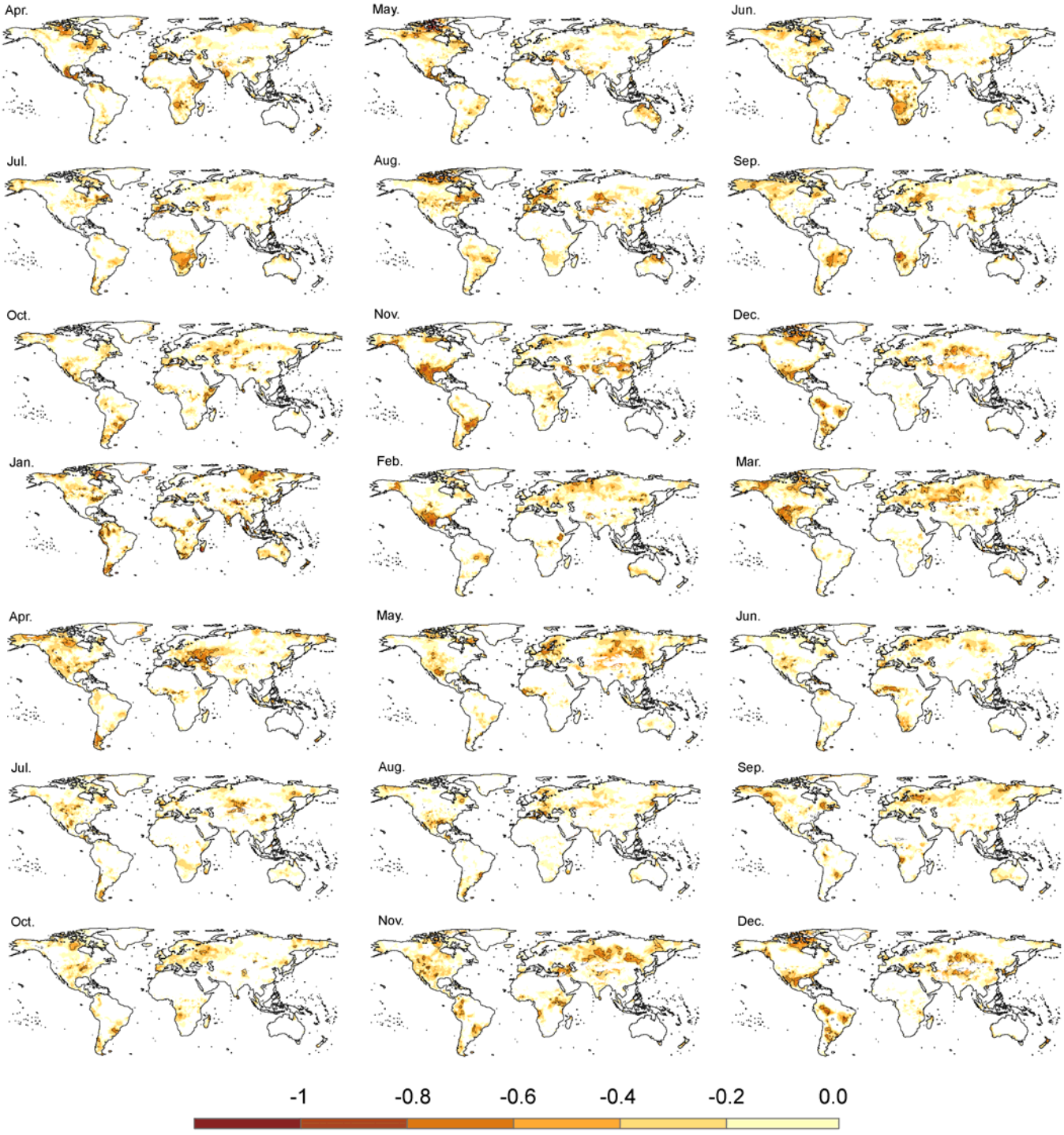
Apr.
May.
Jun.
Jul.
Aug.
Sep.
Oct.
Nov.
Dec.
Jan.
Feb.
Mar.
Apr.
May.
Jun.
Jul.
Aug.
Sep.
Oct.
Nov.
Dec.
-1
-0.8
-0.6
-0.4
-0.2
0.0

Figure 3.

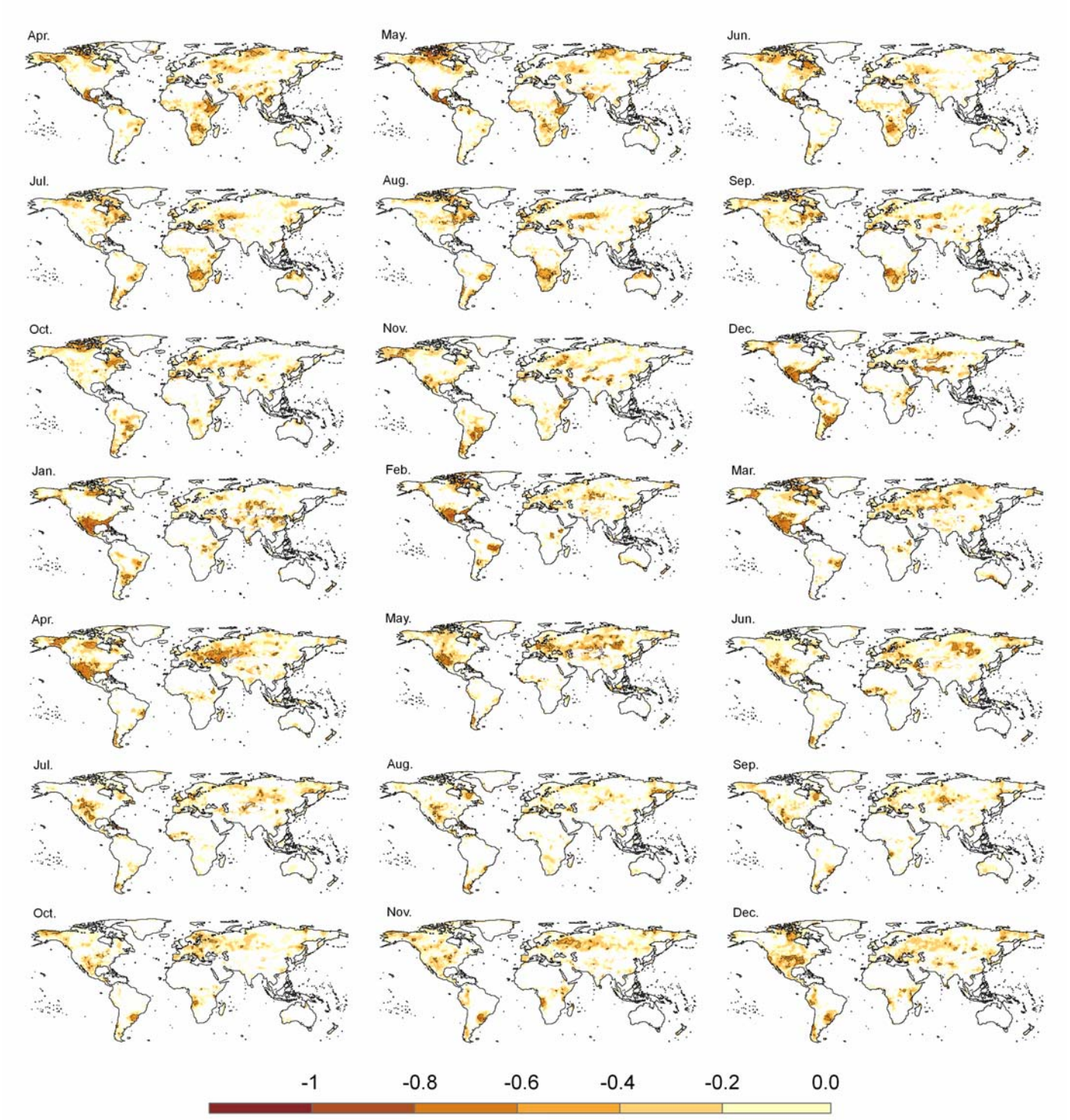
Apr.
May.
Jun.
Jul.
Aug.
Sep.
Oct.
Nov.
Dec.
Jan.
Feb.
Mar.
Apr.
May.
Jun.
Jul.
Aug.
Sep.
Oct.
Nov.
Dec.
-1
-0.8
-0.6
-0.4
-0.2
0.0

Figure 4.

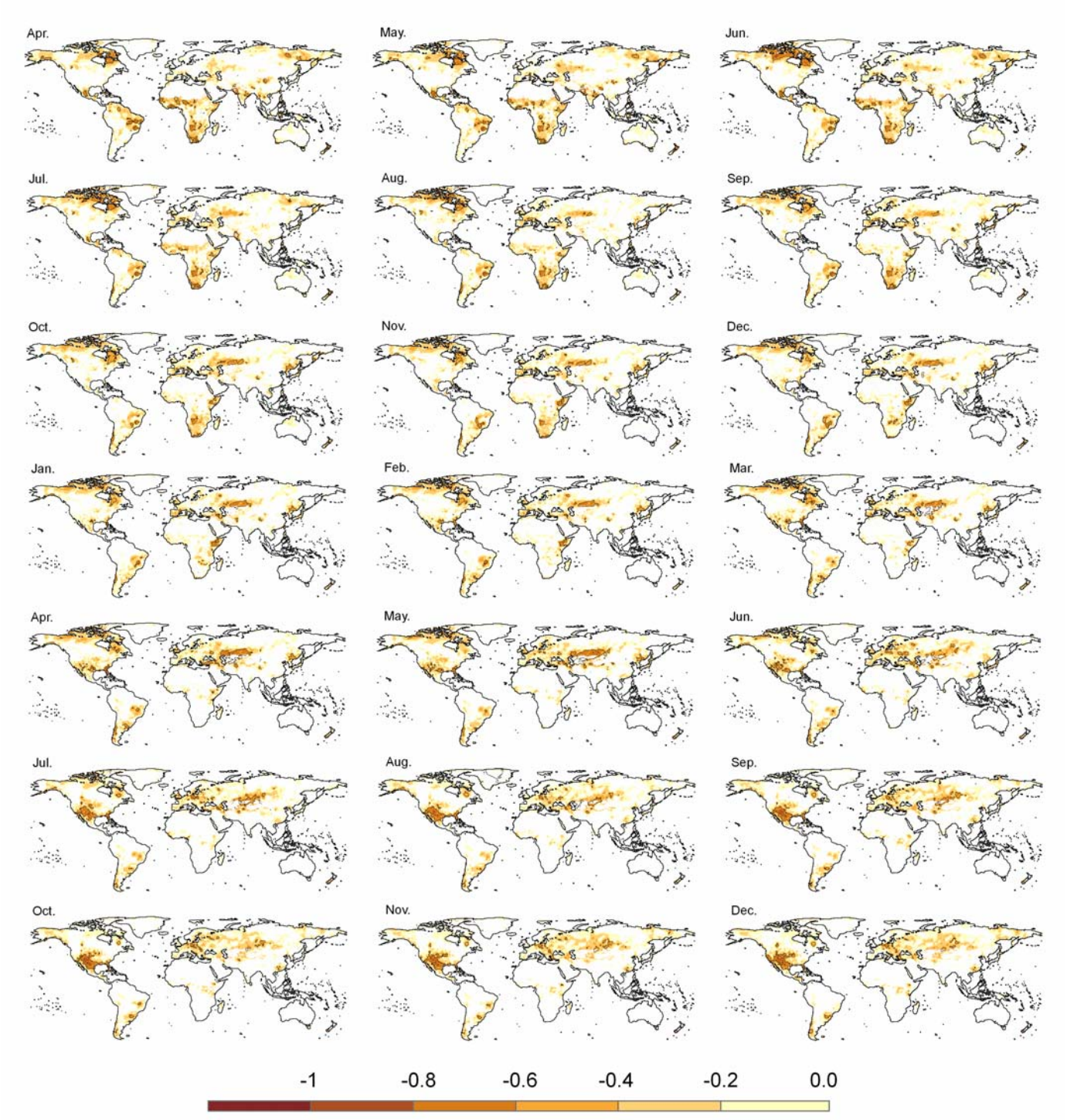
Apr.
May.
Jun.
Jul.
Aug.
Sep.
Oct.
Nov.
Dec.
Jan.
Feb.
Mar.
Apr.
May.
Jun.
Jul.
Aug.
Sep.
Oct.
Nov.
Dec.
-1
-0.8
-0.6
-0.4
-0.2
0.0

Figure 5.

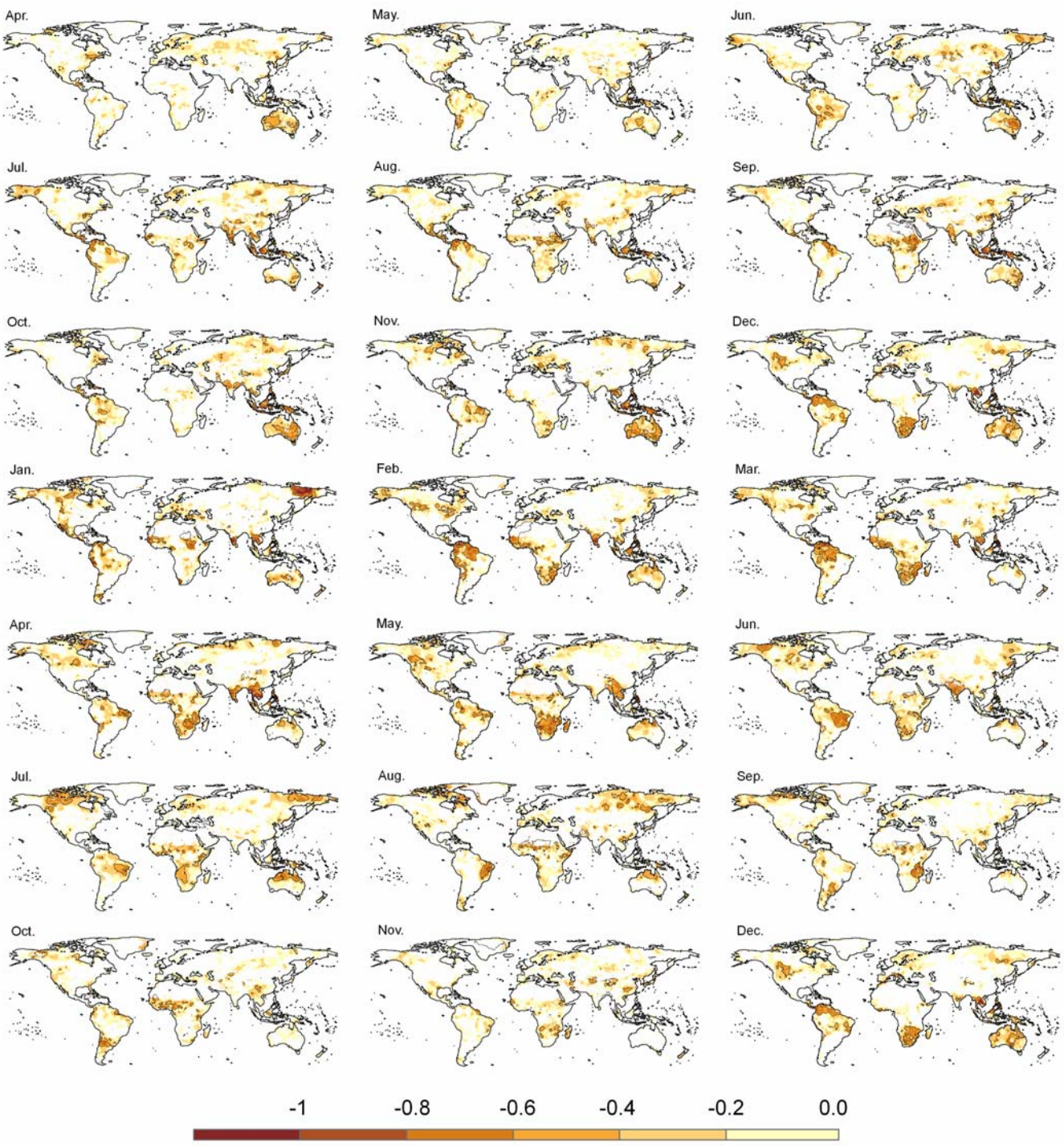
Apr.
May.
Jun.
Jul.
Aug.
Sep.
Oct.
Nov.
Dec.
Jan.
Feb.
Mar.
Apr.
May.
Jun.
Jul.
Aug.
Sep.
Oct.
Nov.
Dec.
-1
-0.8
-0.6
-0.4
-0.2
0.0

Figure 6.

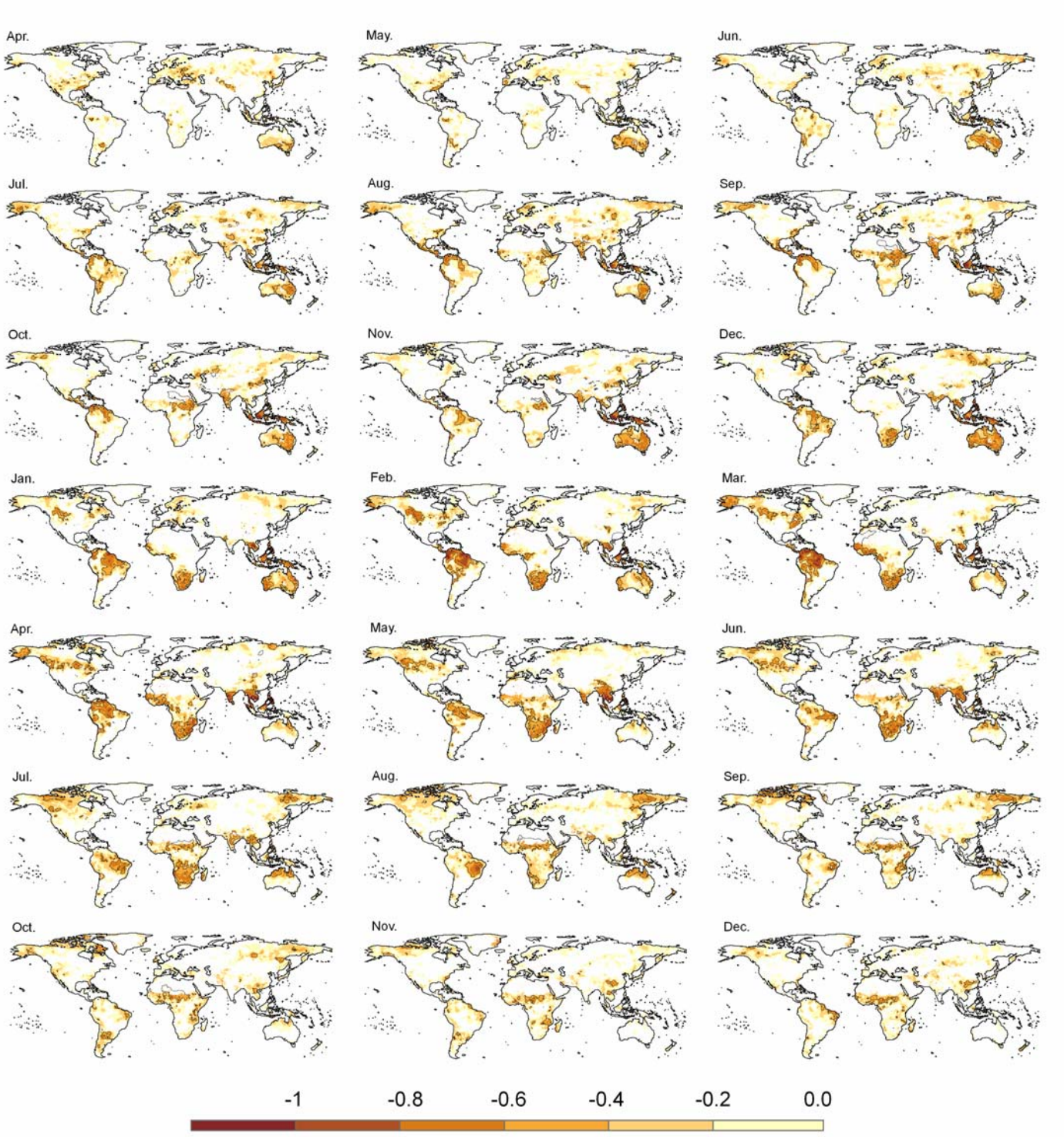
Apr.
May.
Jun.
Jul.
Aug.
Sep.
Oct.
Nov.
Dec.
Jan.
Feb.
Mar.
Apr.
May.
Jun.
Jul.
Aug.
Sep.
Oct.
Nov.
Dec.
-1
-0.8
-0.6
-0.4
-0.2
0.0

Figure 7.

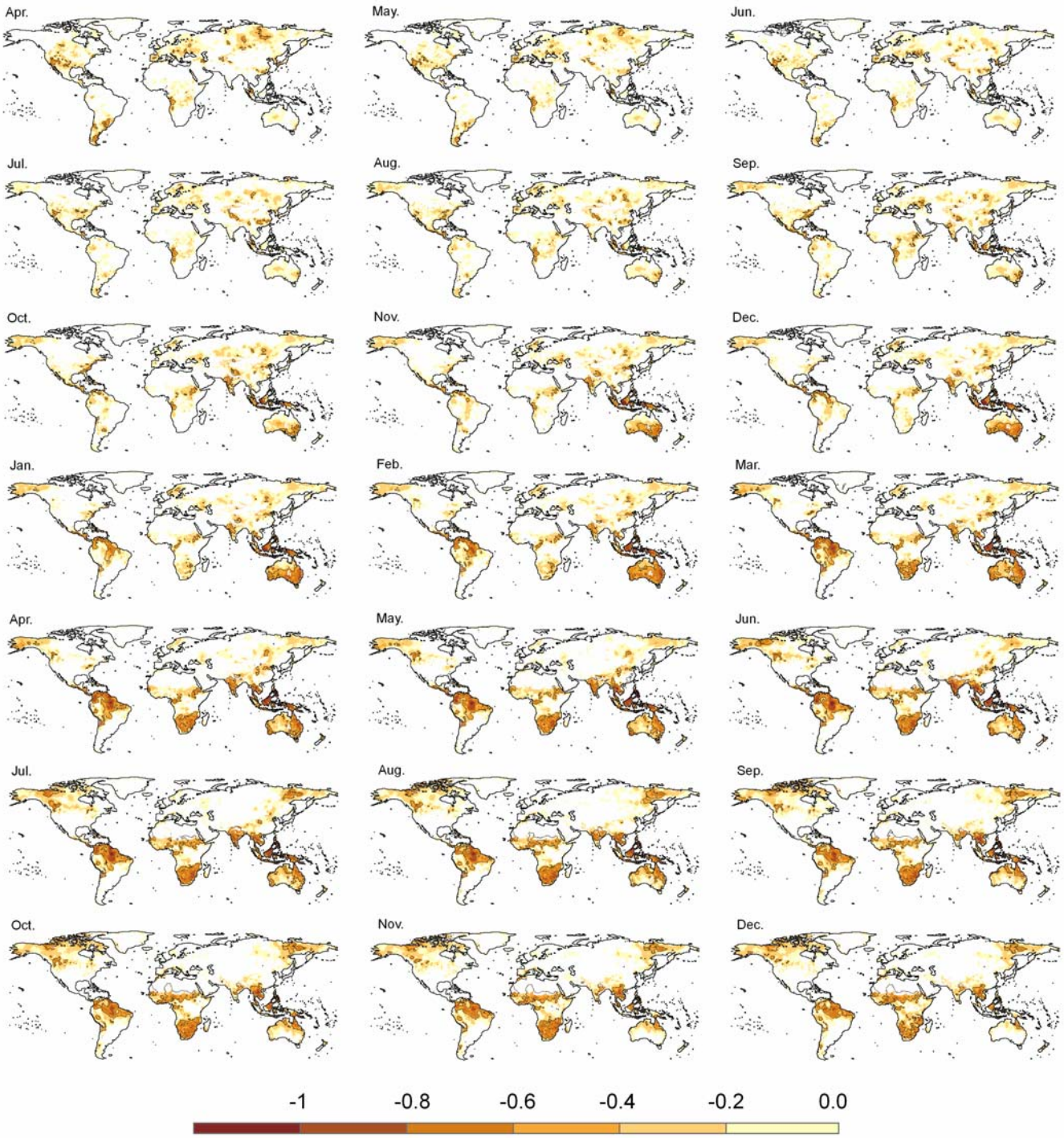
Apr.
May.
Jun.
Jul.
Aug.
Sep.
Oct.
Nov.
Dec.
Jan.
Feb.
Mar.
Apr.
May.
Jun.
Jul.
Aug.
Sep.
Oct.
Nov.
Dec.
-1
-0.8
-0.6
-0.4
-0.2
0.0

Figure 8.

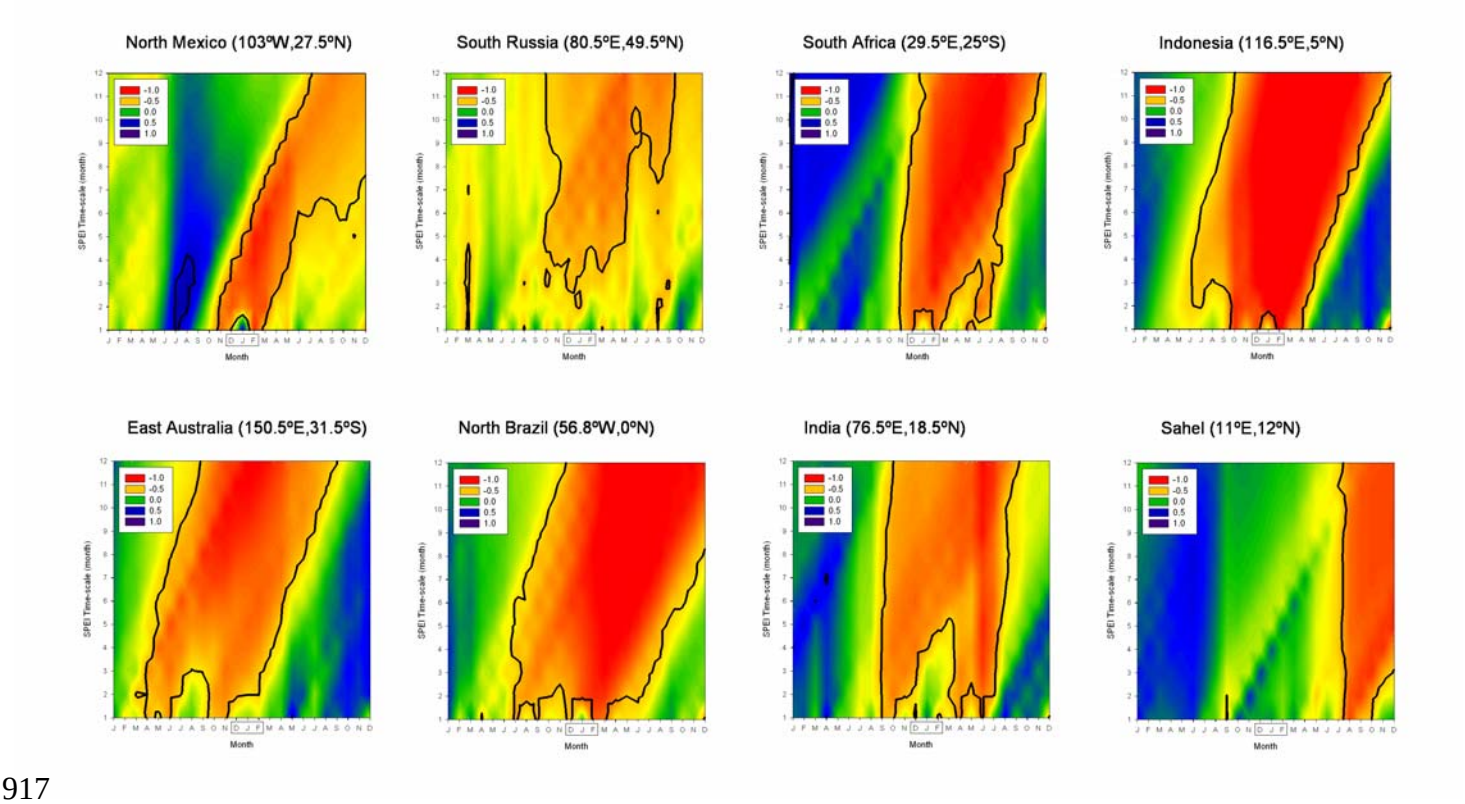
North Mexico (103ºW,27.5ºN)
South Russia (80.5ºE,49.5ºN)
South Africa (29.5ºE,25ºS)
Indonesia (116.5ºE,5ºN)
East Australia (150.5ºE,31.5ºS)
North Brazil (56.8ºW,0ºN)
India (76.5ºE,18.5ºN)
Sahel (11ºE,12ºN)
-1.0
-0.5
0.0
0.5
1.0
SPEI Time-scale (month)
Month
J F M A M J J A S O N D J F M A M J J A S O N D

Figure 9.

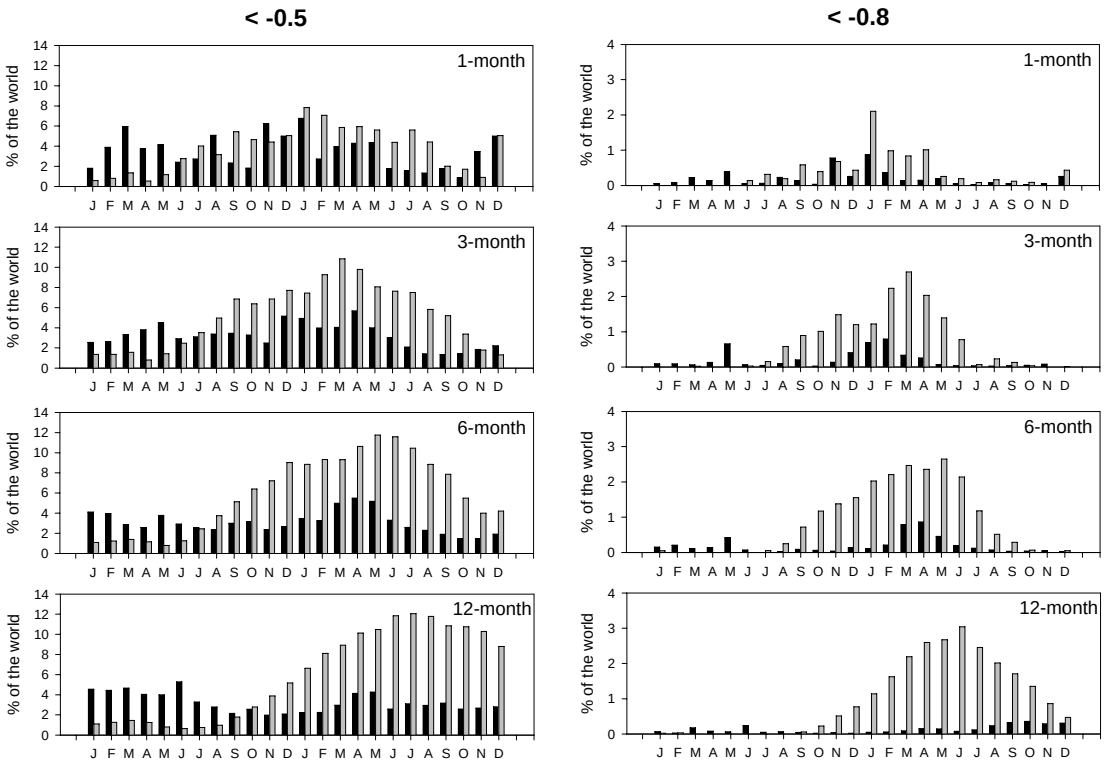
< -0.5
< -0.8
1-month
3-month
6-month
12-month
% of the world
J F M A M J J A S O N D J F M A M J J A S O N D

Figure 10.

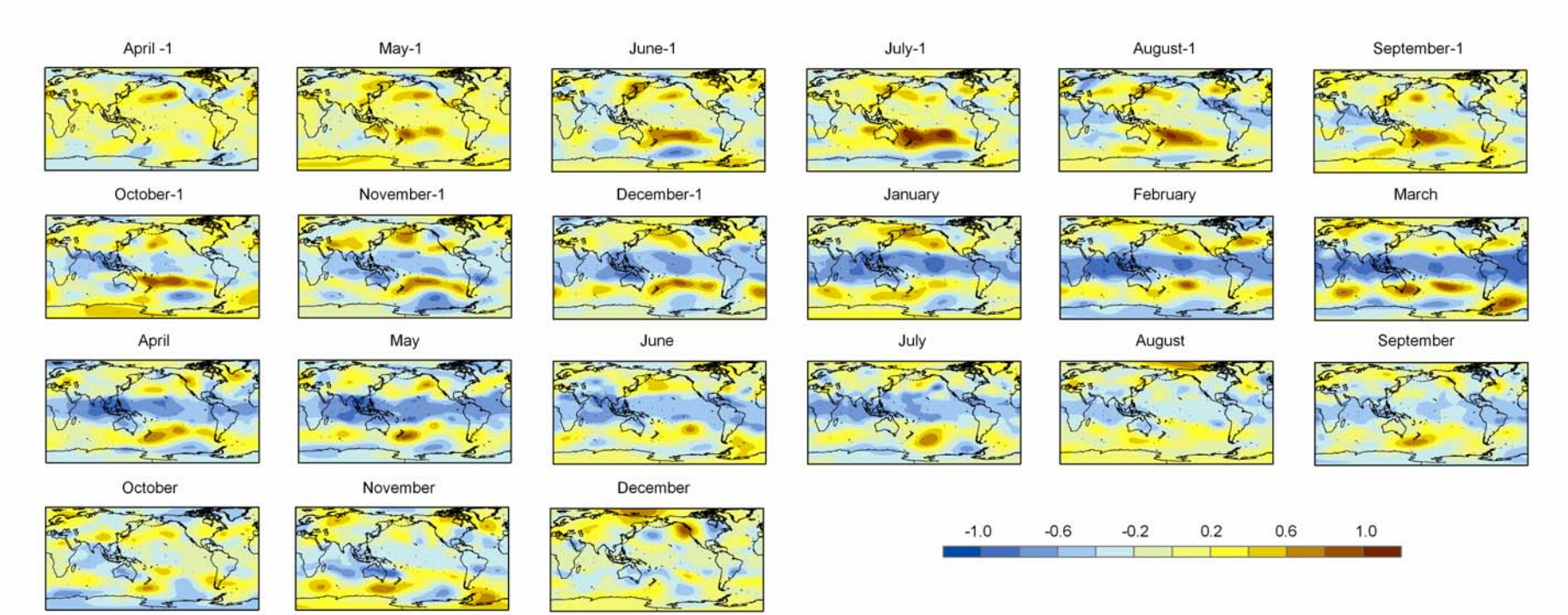
April -1
May-1
June-1
July-1
August-1
September-1
October-1
November-1
December-1
January
February
March
April
May
June
July
August
September
October
November
December
-1.0
-0.6
-0.2
0.2
0.6
1.0

Figure 11.

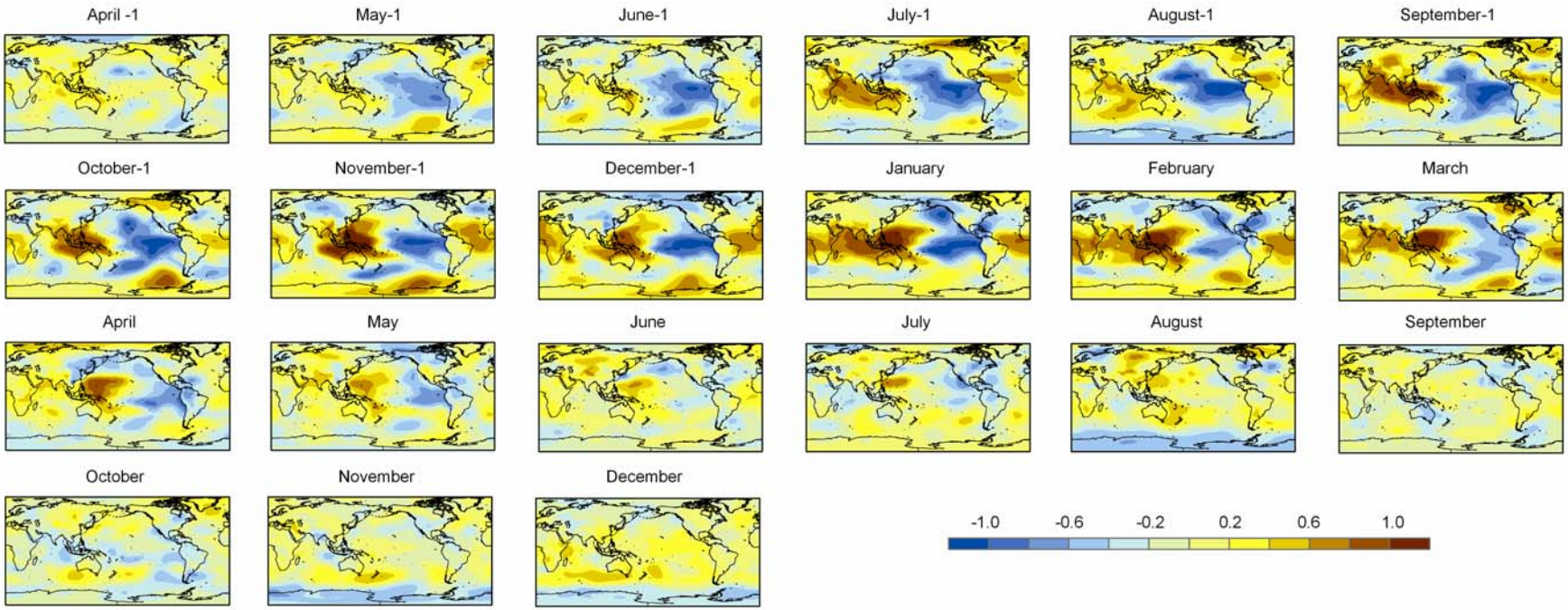
April -1
May-1
June-1
July-1
August-1
September-1
October-1
November-1
December-1
January
February
March
April
May
June
July
August
September
October
November
December
-1.0
-0.6
-0.2
0.2
0.6
1.0

Figure 12.

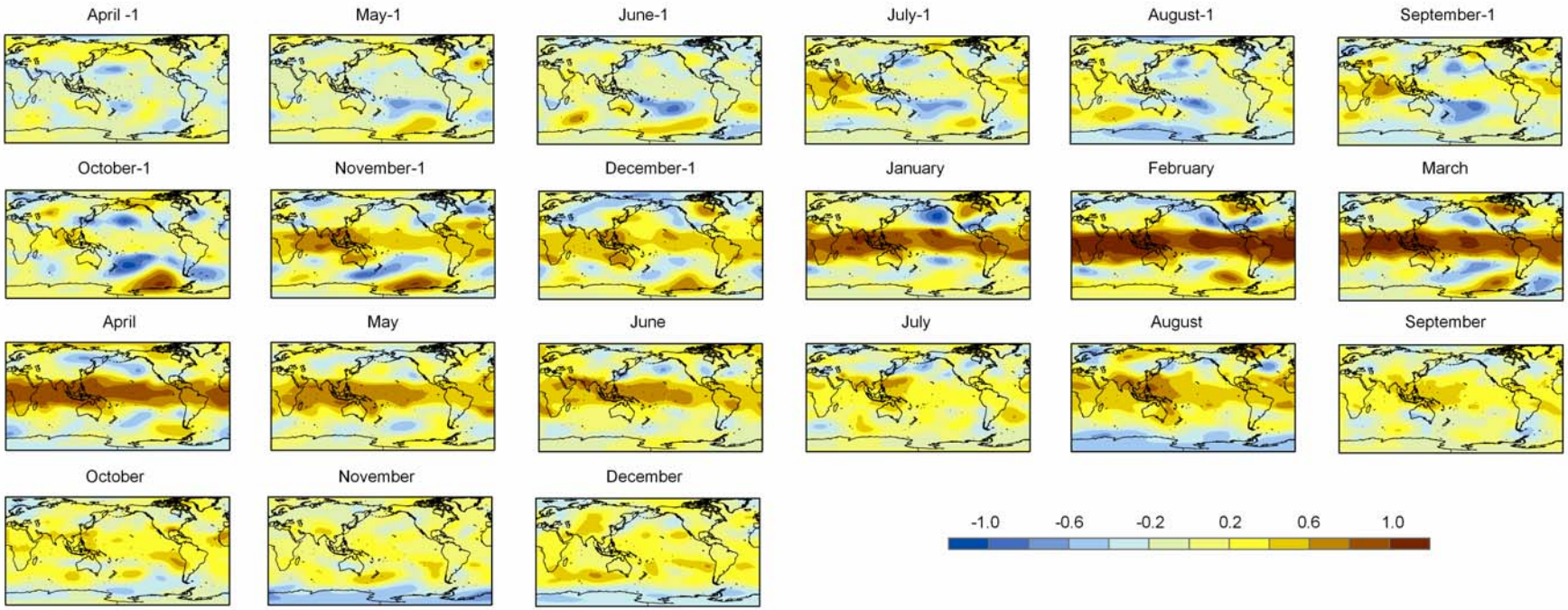
April -1
May-1
June-1
July-1
August-1
September-1
October-1
November-1
December-1
January
February
March
April
May
June
July
August
September
October
November
December
-1.0
-0.6
-0.2
0.2
0.6
1.0

Figure 13: